MACHINE LEARNING & DATA ANALYTICS

FRIEDRICH-ALEXANDER UNIVERSITÄT ERLANGEN-NÜRNBERG
TECHNISCHE FAKULTÄT

Continuous Blood Pressure Measurement During Daily-life Activities Using Pulse Transit Time

Bachelor's Thesis in Medical Engineering

submitted
by

Sophia Leierseder

born 23.02.1995 in Vilsbiburg

Written at

Machine Learning and Data Analytics Lab (Professorship for Computer Science in Sports)
Department of Computer Science
Friedrich-Alexander-Universität Erlangen-Nürnberg (FAU).

Advisors:
Robert Richer M.Sc., Nils Roth M.Sc., Prof. Dr. Bjoern Eskofier
(Machine Learning and Data Analytics Lab, FAU Erlangen-Nürnberg),
Prof. Dr. med. Jochen Klucken
(Department of Molecular Neurology, University Hospital Erlangen)

Started: 15.05.2018

Finished: 12.10.2018

Ich versichere, dass ich die Arbeit ohne fremde Hilfe und ohne Benutzung anderer als der angegebenen Quellen angefertigt habe und dass die Arbeit in gleicher oder ähnlicher Form noch keiner anderen Prüfungsbehörde vorgelegen hat und von dieser als Teil einer Prüfungsleistung angenommen wurde. Alle Ausführungen, die wörtlich oder sinngemäß übernommen wurden, sind als solche gekennzeichnet.

Die Richtlinien des Lehrstuhls für Studien- und Diplomarbeiten habe ich gelesen und anerkannt, insbesondere die Regelung des Nutzungsrechts.

Erlangen, den 9th October 2018

Übersicht

Blutdrucküberwachung kann angewendet werden, um eine Störung der autonomen Blutdruckregulation, die zu einer orthostatischen Dysregulation führen kann, zu erkennen. Obwohl in den letzten Jahren mehrere tragbare Systeme für die Blutdrucküberwachung entwickelt wurden, beeinflussen alle derzeit verfügbaren Geräte die täglichen Aktivitäten der Benutzer.

Bestehende am Handgelenk befestigte Anwendungen schränken die Bewegungsfreiheit der Benutzer ein, indem sie eine bestimmte Armposition voraussetzen. Eine solche Voraussetztung wird getroffen, da die Blutdruckwerte durch den hydrostatischem Druck beeinflusst werden, der sich mit der Armposition ändert. Diese Einschränkung setzt eine aktive Beteiligung voraus und kann zu einer Verfälschung der Blutdruckergebnisse aufgrund menschlicher Fehler führen. Aus diesem Grund wird in dieser Arbeit ein System zur Armpositionserkennung vorgestellt, das als Grundlage für ein Blutdrucküberwachungssystem zur unauffälligen Blutdruckmessung ohne Einschränkung der Armbewegung des Benutzers dient.

Die Erkennung der Armposition basiert auf Daten eines dreiachsigen Beschleunigungsensors, eines Dreiachsengyroskops und eines Barometers. Die erfassten Sensorsignale werden mit einem entwickelten Algorithmus verarbeitet, der die Armposition des Benutzers bestimmt. Die Leistung der Armpositionserkennung wurde in einer Studie, an der 15 gesunde Testpersonen teilnahmen mit einer Genauigkeit von 94,44 %, einer Precision von 94,51 %, einem Recall von 94,44 % und einem F1-Score von 94,46 % bewertet. Die Ergebnisse zeigen, dass die vorgestellte Sensoreinheit und der Algorithmus aussagekräftige Daten für eine nachfolgende Anpassung der Blutdruckwerte durch die Armposition des Benutzers liefern.

Abstract

Blood pressure monitoring can be applied to detect disorders of the autonomic blood pressure regulation, which may lead to orthostatic dysregulation. Even though several unobtrusive wearable systems for blood pressure monitoring were developed in recent years, all currently available devices affect users' everyday activities.

Existing wrist-worn applications restrict users in their freedom of arm movement by requiring a specific arm position. Such a presumption is made because the blood pressure values are influenced by the hydrostatic pressure, which changes with the arm position. This requirement of users' active involvement may lead to falsification of blood pressure results due to human error. For this reason, this thesis presents a system for arm position detection, building the basis a wrist-affixed system for unobtrusive blood pressure estimation without any limitation of users' arm movement.

Arm position detection is based on sensor data from a three-axes accelerometer, a three-axes gyroscope and a barometer. The acquired sensor signals are processed with a developed algorithm determining the user's arm position. The performance of the arm position detection is evaluated using 15 healthy test persons, providing an accuracy of 94.44 %, a precision of 94.44 %, a recall of 94.64 % and a F1-score of 94,46 %. The results demonstrate that the presented sensor unit and algorithm provide valuable data for the adjustment of blood pressure values by users' arm position.

Contents

Chapter 1

Introduction

Monitoring physical functions serves as an important indicator for the assessment of a person's state of health [Hol17]. In particular, a dysfunctional cardiovascular activity can be an evidence for illness [Lud17]. The arterial blood pressure, which is the outcome of arterial resistance and cardiac output, is a key indicator used in the assessment of cardiovascular system performance [Hol17].

A disorder in blood pressure regulation can be determined during a change of posture. If a person abruptly changes posture, e.g.an from a lying to a standing posture, part of the blood sags into the legs and the abdominal cavity [Ric16]. A healthy cardiovascular system reacts by tightening the blood vessels and increasing the heart rate to maintain the blood pressure constant, after a short blood pressure increase [Hae05]. Failure of this regulatory mechanism will cause dizziness, short-term drowsiness, and sometimes even syncope. If a patient complains about these symptom, this could be an indication of Parkinson's disease [Mih06]. Parkinson's disease affects the motoric system and causes disorders in the autonomic blood pressure regulation, leading to orthostatic dysregulation. Due to autonomic failure in idiopathic Parkinson's disease, blood pressure of a Parkinson's patient will decrease more strongly after changing posture, compared to a healthy person's blood pressure [Pic05].

Among other things, for the definite diagnosis of Parkinson's, it is necessary to monitor the autonomic blood pressure regulation of the patient. In the hospital, an invasive method where a catheter is inserted into a patient's artery, is often used to continuously measure arterial blood pressure. This method is considered as the most precise method and is therefore known as gold standard. However, the performance of the measurement depends greatly on the abilities of the doctor or the medical staff. Additionally, invasive measurement is associated with pain and risk [He14]. These techniques are neither practical nor appropriate for repeated measurements

in non-hospitalized patients. Due to these massive disadvantages, cuff-based methods for blood pressure measurements were
invented [Din16].

Cuff-based devices detect oscillations during cuff-inflation using a built-in pressure sensor [Sha17]. There are clinical standard tests to determine orthostatic dysregulation, where cuff-based methods are applied, including the Schellong test and the Tilt Table Test. In both tests, blood pressure and pulse are measured with cuff-based devices [Per93]. Unfortunately, it may happen that these tests are negative and no malfunction of the circulatory system is diagnosed, an indication of Parkinson's disease is present. On the one hand, this might occur due to the White Coat syndrome, which implies that the patient's blood pressure and heart rate is higher in a clinical surrounding than in a home environment [Owe99]. In case of this syndrome, no blood pressure decrease can be determined after a posture change, due to a naturally higher blood pressure in a clinical surrounding. Hence, it is beneficial to monitor blood pressure unobtrusively in a home environment in order to reduce environmental influences on the patient's physiology, and increase the quality of results and the patient's comfort [Din16]. On the other hand, a reason for a misdiagnosis could be that in the Schellong and the tilt table test only snapshot measurements of blood pressure and pulse can be measures. There is a possibility that within this short period of time pathological changes in blood pressure regulation can be observed [Owe99] [Ges12]. Therefore, there is a need for continuous blood pressure monitoring over a long period of time and in a home monitoring setting.

There are already some existing cuff-less devices for unobtrusive blood pressure monitoring, which are based on the measurement of pulse transit time since previous work has shown a correlation between pulse transit time and blood pressure [Ged81]. In general, pulse transit time is defined as as the time the pulse wave needs to travel between two points of the cardiovascular system [Hol17]. One specification of pulse transit time is the time delay between the R-wave of an electrocardiogram (ECG) and the arrival time of the blood pressure wave on a finger, which is determined by a photoplethysmogram (PPG) [Ges12]. The ECG signal reflects the electrical activity of the heart, while the PPG signal consists of pulses that reflect the change in vascular blood volume within each cardiac beat [Tho16]. Building on pulse transit time based methods, it is possible to measure blood pressure unobtrusively and continuously and thus increase the daily-life usability [Car17a].

However, a problem of pulse transit time based methods is that the correlation between pulse transit time and blood pressure is highly influenced by changes in hydrostatic pressure, which is dependent on the user's arm position [Din16]. Typically, blood pressure measurement is

referenced to the proximal
aorta [Sha08]. This implies that the blood pressure measurement is performed while the arm is at the height of the heart in order to eliminate the influence of hydrostatic pressure. Thus, the hydrostatic effects cause errors in case a blood pressure measurement is made with a finger-fixed PPG sensor and the finger is at a position higher or lower than the heart [Sha08]. In order to enable users' unrestricted arm movement, blood pressure measurement systems should detect the user's arm position automatically and without further actuation [Sha08]. Hence, this thesis presents and verifies a sensor system for arm position detection in wrist-worn blood pressure measurements devices. The systematic solution aims to refine existing systems and make the blood pressure measurement as unobtrusive and pleasant as possible. It further allows for an accurate calibration of blood pressure for different arm positions. In order to detect the different arm positions, the PPG sensor is equipped with an inertial measurement unit (IMU), consisting of accelerometer and gyroscope, and a barometer that measures atmospheric pressure.

This bachelor's thesis consists of two topics, which are treated separately: (1) blood pressure estimation based on pulse transit time and (2) arm position detection. In order to calculate the pulse transit time, an algorithm based on the ECG signal and the PPG signal is developed. The ECG signal is recorded with two electrodes, while the PPG signal is obtained with a finger-worn sensor. An algorithm based on accelerometer, gyroscope and barometer signals performs the arm position detection. Finally, data of 15 healthy subjects is collected in order to evaluate the feasibility of the presented system.

Chapter 2

Related Work

2.1 Blood Pressure Measurement

Blood pressure is one of the fundamental monitoring parameters in medicine [Sha17]. In 1847, an invention of Carl Friedrich Wilhelm Ludwig enabled the measurement of blood pressure for the first time [Boo77]. He developed a kymograph, which was used to record continuous vibrations of the human arterial pressure. The pressure was determined using a cannula, which was located in an artery [M. 87] [Din16].

About one hundred years later, intra-arterial blood pressure monitoring through an arterial line became the new standard method for blood pressure measurement [Pet48]. It allowed recording blood pressure over a longer period of time [Din16]. This method included a small plastic catheter filled with a fluid column, which was inserted into the artery. The arterial pressure waveform was transferred from the fluid column to a converter. There, the recorded signal was converted into an electrical signal, which could be displayed on a terminal [Din16].

First efforts towards non-invasive blood pressure monitoring already existed before. Since 1881, it was possible to measure blood pressure with a sphygmomanometer, which consists of an inflatable cuff wrapped around the upper arm to compress the artery, and an attached manometer [Boo77]. Riva Rocci improved this procedure in 1896 by adding a branchial cuff sphygmomanometer [Sha17].

In 1905, the detection of Kortokoff sounds in combination with the sphygmomanometer enabled a completely non-invasive blood pressure measurement [Kor05]. Nevertheless, this method still required the presence of a medical expert [Sha17]. Moreover, it only allows snapshot blood pressure measurements and is therefore not applicable for continuous blood pressure monitoring.

In 1963, Pressman and Newgard introduced a non-invasive blood pressure measurement method based on arterial tonometry [Drz83]. It is based on the principle that the pressure in an artery is similar to the force that is required to flatten the artery's surface [Che13]. Due to this method, it was possible to measure blood pressure without the involvement of medical staff. However, the method requires unhandy equipment which does not allow to apply this method in a home monitoring setting.

Since devices are not suitable for home-based and continuous blood pressure measurement, oscillometry-based tools have increased in popularity. They are neither invasive nor require medical staff to operate and hence, can be used to monitor blood pressure in the home setting [Sha17]. Oscillometry is based on the detection of oscillations of the lateral walls of the artery, while device's cuff is inflated [Per93]. The main disadvantage of oscillometry-based devices is the significant distortion of the measuring results through movements[Lin15].

In 1973, Penaz et al. developed a technique which did not injure the patient by arterial catheterization, but still offers the benefits of continuous blood pressure monitoring. Penaz invention is based on the volume-clamp method which assumes that the cuff pressure is equal to arterial pressure [Chu13]. Basically, the device consists of a finger cuff with an integrated photoplethysmograph [Pen92]. The system is able to determine the blood volume in the finger via infrared light absorbance [Chu13]. This technique has been modified by Finapres and is available as a commercial product for non-invasive continuous blood pressure measurement [Sha17]. Because measurements via arterial line are considered as too invasive for regular clinical use, this method is considered as the gold standard for continuous blood pressure measurement[Che13].

Although the oscillometer made home-based blood pressure measurement possible, due to unhandiness this method still affects the user's daily life. For this reason, these methods have been superseded in recent decades by unobtrusive devices [Sha17], allowing long-term monitoring in a home setting [Bon10]. In recent years, there were various approaches to measure blood pressure non-invasively and without a cuff [Din16].

One approach was a wearable sensor patch system that integrates flexible piezoresistive sensors (FPS) and epidermal ECG sensors for cuff-less blood pressure measurement [Luo16]. Another noninvasive long-term blood pressure measurement method continuously records blood pressure on the user's wrist using ultrasound, a small balloon and a controller [Web13].

However, the most common way to measure blood pressure unobtrusively is to estimate blood pressure by calculating the pulse transit time and correlate it with blood pressure recordings obtained by a reference device [Din16]. Previous work mostly required an ECG sensor, which is attached to the wrist and a PPG sensor, which is usually attached to a finger to compute pulse

transit time. There are some approaches, such as BioWatch, where both sensors are located at the wrist [Tho16]. Due to the fact that the ECG signal is recorded across the heart both hands of the user and two electrodes are needed to measure the pulse arrival time. One electrode is on the bottom side of the watch, making contact with the left arm, whereas the second electrode is located on the top of the watch. The user wears the device on the left hand and touches the ECG electrode with the right hand to complete the electrical connection for the ECG.

Another approach using pulse transit time for blood pressure estimation is SeismoWatch, presented by Carek et al. [Car17b]. They developed a wrist-worn blood pressure monitor which measures blood pressure while holding the device against the user's sternum to record a seismocardiogram (SCG), micro-vibrations of the chest wall associated with the heart beat. An accelerometer and an optical sensor mounted on the watch measure the pulse transit time as a pulse wave, diffusing from the heart to the wrist. In order to record the SCG signal, the device has to be pressed against the sternum.

Holz et al. presented another pulse transit time based approach [Hol17]. They proposed an eyeglass equipped with several PPG sensors for the computation of the pulse transit time between different arteries in the head. Their method allows the passive estimation of blood pressure without any need for interaction. However, this method requires users to wear conspicuous eyeglasses.

There are further applications and patents for blood pressure measurement by means of pulse transit time [Oh08] [Mat10] [McC10a]. The accuracy of all listed applications for blood pressure measurement with pulse transit time is limited due to several challenges [Bux15]. One particular challenge for pulse transit time based devices located at the patient's wrist is the elimination of the hydrostatic pressure, which affects blood pressure results and is dependent on the user's arm position [Sha08].

2.2 Arm Position Detection Methods

The PPG signal is usually measured on the wrist or on the finger. If these body parts are not at heart level, the hydrostatic pressure influences the PPG signal [Sha17]. Therefore, the system has to be extended in order to include all potential arm positions and eliminate the falsification of results caused by the hydrostatic pressure.

An initial attempt to obtain a method for estimating individualized coefficients for pulse transit time measurement was made by Poon et al. in 2006 [Poo06]. Poon modeled pulse transit time under the effects of hydrostatic pressure due to hand lifting. However, no automatic arm position recognition was possible with this method.

The blood pressure measurement method of Shaltis et al. automatically detects the arm position [Sha08]. The height of the blood pressure sensor is estimated using two accelerometers: one accelerometer approximates orientation of the upper arm relative to gravity; the other receives the approximate orientation of the lower arm. With these orientations and the knowledge of the lengths of the humerus and the lower arm segment of a person, it is possible to calculate the height of the hand using standard trigonometry [Sha08]. For that reason, Shaltis' approach is not generally applicable for everyone because the lengths of upper and lower arms need to be precisely measured before usage.

In the paper BioWatch, which was already mentioned, a system that is able to detect the user's arm position at chest level is presented [Tho16]. In comparison to the device presented in this thesis, the arm-position detection method of Thomas et al. is solely based on an accelerometer. Due to limitations of the accelerometer and due to the fact that the user has to wear the application on the one arm and touch the application with a finger from the other hand, BioWatch allows measurements only in a limited range of arm positions[Tho16]. This systematic restriction limits the usability of BioWatch during daily life activities.

The presented work related to blood pressure estimation and arm position detection illustrates that intense research has been conducted in this domain during past years. Some existing patents for arm position detection already exist, e.g. as presented by Michael J. Golden [Gol99]. There are systems that perform blood pressure estimation based on pulse transit time while considering the user's arm position, blood pressure with pulse transit time measurement and considering the users' arm position [McC10b] [Har10].

However, none of them meets the requirements for daily-life usability. This bachelor's thesis pays special attention to the development of an arm position detection system without limitations regarding arm movement, utilizing an accelerometer, a gyroscope and a barometer.

Chapter 3

Fundamentals

This section describes the theoretical background of blood pressure regulation in the cardiovascular system, the blood pressure measurement using pulse transit time (PTT) or pulse arrival time (PAT) and the influence of hydrostatic pressure on blood pressure results. Since a blood pressure regulation malfunction is the motivation of this thesis, the processes that occur in such a malfunction are explained in more detail. In this thesis particular attention is paid to the application's arm position detection to eliminate the effect of hydrostatic pressure. Due to this fact, it is essential to define hydrostatic pressure and its influence on blood pressure results.

3.1 Blood Pressure Regulation

Depending on the temporal occurrence of action, a distinction is made between mechanisms of short-term and long-term blood pressure regulation. The short-term regulation of blood pressure primarily serves pressorceptors in the large thoracic and cervical vessels, in particular in the branching of the carotid artery (carotid sinus) and on the aortic arch. Long-term blood pressure regulation is primarily a function of the fluid balance [Lan07]. In order to keep the blood pressure constant The perfusion of individual organs can be reliably adjusted by appropriate changes in vascular resistance as long as the systemic blood pressure is maintained. In particular, if the blood pressure is too low, the brain can no longer be adequately supplied with blood which will cause dizziness. Conversely, a too high blood pressure may damage vessels and may eventually threaten the function of the heart. Therefore, normal blood pressure regulation is of the utmost importance and is associated with the monitoring of blood pressure. Several control mechanisms are used to keep the blood pressure at the required level. Figure3.1 shows how the parameter of blood

pressure regulation should behave in the event of a sudden change of posture. If these mechanisms fail, it has to be recognized as soon as possible [Lan07].

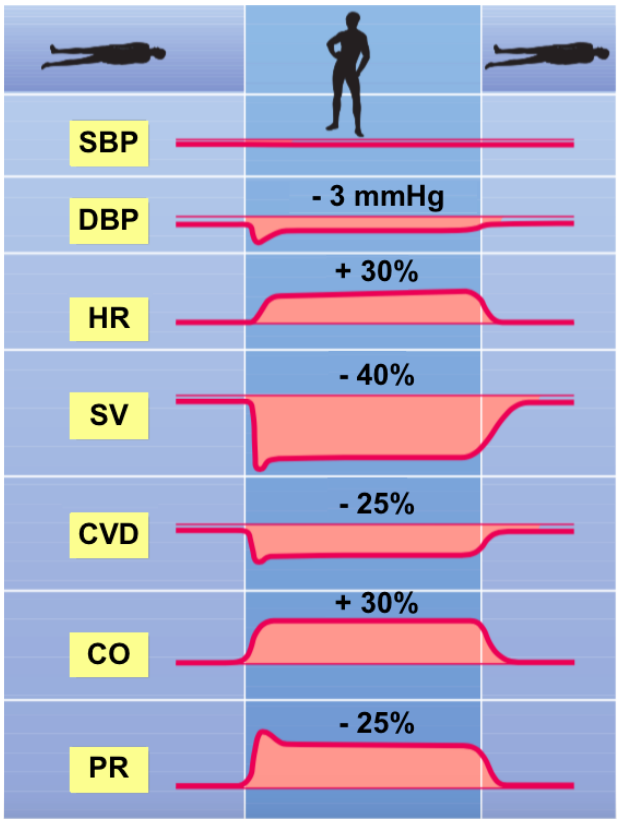

Figure 3.1: **Regulation mechanisms of the cardiovascular system after a posture change from lying to standing:** systolic blood pressure (SBP), diastolic blood pressure (DBP), heart rate (HR), stroke volume (SV), central venous pressure (CVD), cardiac output (CO), peripheral resistance (PR) [Lan07]

3.2 Blood Pressure Measurement

As already mentioned, the basis of this work is the inconspicuous estimation of blood pressure fluctuations by measuring the PAT. At this point, the terms PAT and PTT and their process are explained in more detail. PAT is inversely related to blood pressure (see Equation 3.1) [Muk15]. As Mukkamala et al. describe in

$$BP = \frac{K1}{PTT + K2} \quad . \tag{3.1}$$

PAT is the amount of time it takes a blood pressure wave generated by the beat of the heart to travel down the arterial tree to a point of the body. It is necessary to measure two specific events that occur in the body in order to determine PAT: the heart beat and the arrival of the pulse wave at a specific location of the body.

The typical method of determining the heart beat is to provide the person with electrodes to measure their ECG and monitor when their heart is beating by recording the R-wave [Sha08]. Potential changes in the heart cells produce dipoles that create potential deflections on the skin surface. These deflections are detected by the ECG. As already mentioned the peak relevant to the PAT is the R-peak. This is the first positive peak that arises in the excitation propagation in the chamber [Lan07].

Besides the ECG sensor an optical pulse sensor is applied to the person. This measures the PPG at the fingertip [Hol17]. Thereby, infrared light is emitted into a selected part of skin, depending on the blood volume more or less light is absorbed. As a result, blood volume changes be determined by measuring the reflected light [Shr10].

The problem with blood pressure estimation using PAT is that the R-peak does not capture the exact moment when the blood is actually dropped out from the heart, but rather when the heart depolarizes at the onset of a contraction. Therefore, measurement of PAT is inherently noisy [Hol17]. To circumvent this problem, the variable rejection period must be counteracted, which causes the noise. This is achieved by using the PTT instead of the PAT. PTT is the time delay for the pressure wave that follows a heart beat and is also inversely proportional to blood pressure. The PTT measurement differs from the PAT in that different arterial events are used to determine the timestamp at a proximal site [Muk15].

3.3 Hydrostatic Pressure

If the PAT or PTT are determined by a, there is an effect on blood pressure results due to the hydrostatic pressure. Hydrostatic pressure is the pressure that occurs within a fluid like blood, due to the influence of gravity [Lan07]. Blood pressure measurements are usually referenced to the proximal aorta, the hydrostatic pressure is assumed to be zero there. The reference to the proximal aorta is usually provided when using the R-peak from the ECG signal as initial point for PAT measurement. Since the PPG sensor is usually attached to the wrist or finger, the signal depends on the position of the arm. If the PPG measurement is performed at a location that is higher or lower than the heart, hydrostatic effects will cause an error [Sha08]. In order to eliminate such errors, the arm position has to be detected to calculate BP correctly.

Chapter 4

Methods

The objective of this thesis is to create an algorithm for arm position detection, in order to eliminate the hydrostatic error on estimated blood pressure values. Therefore, the processing pipeline illustrated in Figure 4.1 is applied. The thesis subdivided into two subparts. The first subpart is the blood pressure estimation based on the calculation of PAT. The second subpart constitutes the arm position detection. A combination of both subparts enables obtaining correct blood pressure values.

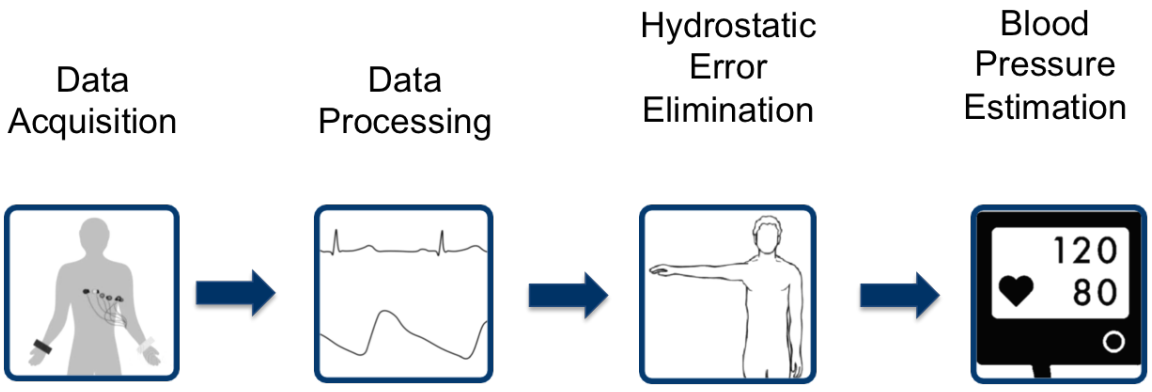

Figure 4.1: **Processing Pipeline for blood pressure estimation using PAT:** Various signals are recorded to calculate the PAT values and eliminate their hydrostatic error.

At first, the data for PAT calculation and arm position detection is gathered. As previously mentioned, PAT is defined as the time delay between the R-peak of an ECG and the arrival of the pulse wave at a limb apparent from a PPG [Ges12]. Both ECG and PPG signals for PAT computation as well as accelerometer, gyroscope and barometer data for arm position detection were streamed to a smartphone via Bluetooth®. The recording of all mentioned signals starts

simultaneously after the user activates a start button. All data are logged to the external storage for the data processing step.

4.1 Blood Pressure Estimation

The first part of the thesis consists of the PAT calculation, which is correlated with blood pressure values. Therefore, the following section details the hardware for the data acquisition and the data processing steps for PAT calculation. An overview of the processing pipeline for blood pressure estimation is visualized in Figure 4.2. The regression parameters for the elimination of the hydrostatic error originate from a calibration procedure. The arm position detection ensures that the correct parameters for the respective arm position are used and is described in Chapter 4.2.

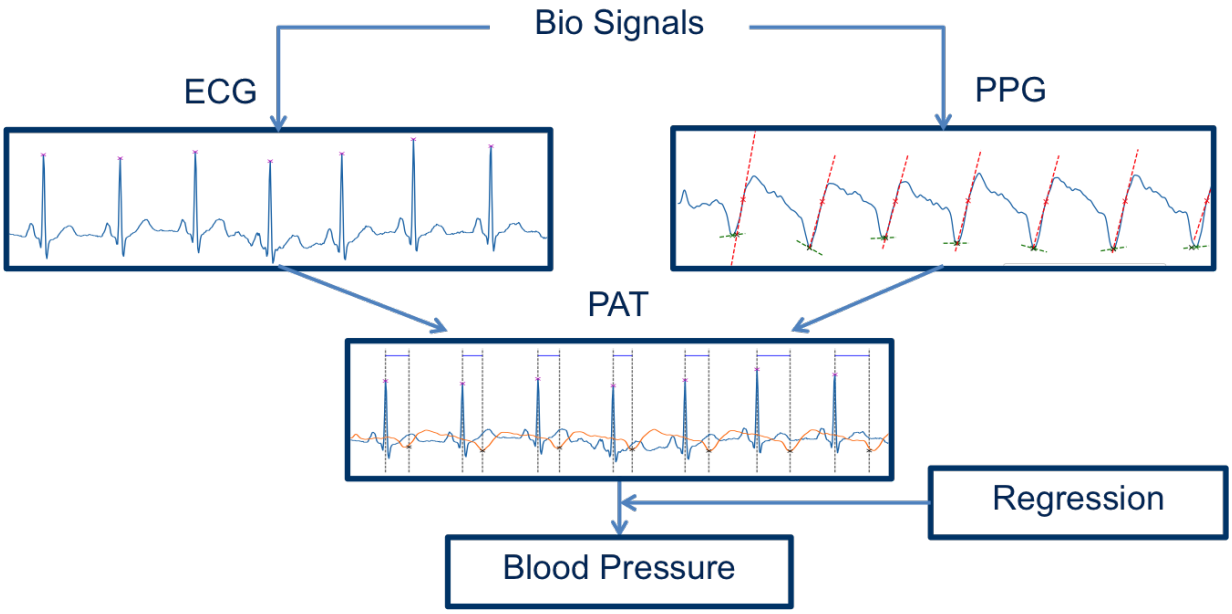

Figure 4.2: **Processing pipeline for blood pressure estimation:** The ECG and the PPG signals are required to calculate the PAT. The PAT is affected by hydrostatic effects, these are eliminated with regression parameter.

4.1.1 Data Acquisition

Notwithstanding the hydrostatic pressure, two bio signals are necessary for the PAT calculation: the ECG and the PPG. These signals are recorded simultaneously using two different sensors. Figure 4.3 shows the sensors placement to obtain the required signals.

Figure 4.3: **Sensor attachment:** The ECG sensor is attached with two electrodes, which are placed at the top of the sternum and at the left anterior axillary line. The PPG sensor is attached to a finger on the left hand and connected to the arm position detection sensor unit on the left wrist.

The ECG signal is recorded with the sensor system illustrated in Figure 4.4. With two electrodes and a sampling frequency of 25 Hz, a 1-channel ECG signal is recorded. In order to A 1-channel ECG signal was recorded at a sampling rate of 125 Hz with two electrodes placed according to Lead II of Einthoven's Triangle, both electrodes are attached to the proband's body, as shown in Figure 3.

The PPG signal is recorded with an existing sensor system and is illustrated in Figure 4.5. It is important to ensure that the sensor is installed in the housing so that the LEDs are in contact with the skin to make a PPG recording possible. It is equipped with a red LED and an infrared LED. Both LEDs enable a recording of a PPG signal of 250 Hz. In this bachelor's thesis the infrared light LED is used for further applications.

Figure 4.4: **ECG sensor:** Hardware of the ECG sensor, including the circuit board, the battery and two leads for the electrodes

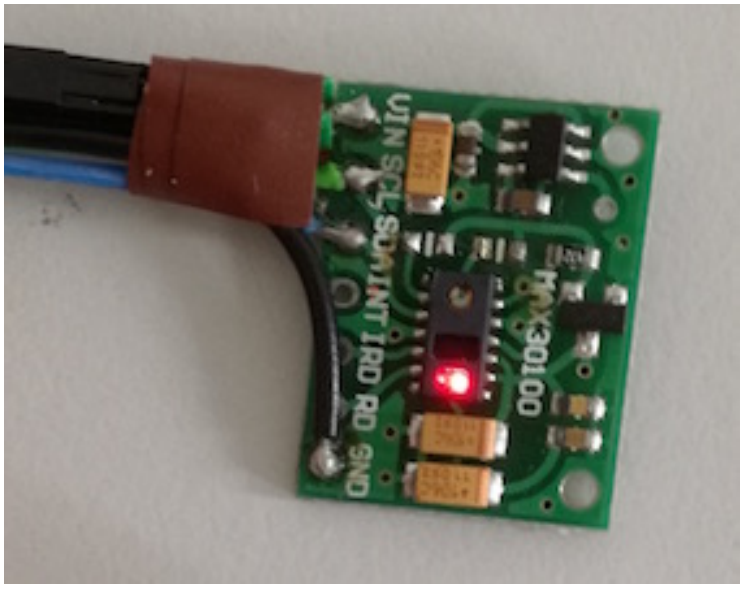

Figure 4.5: **PPG sensor:** Circuit board of the PPG sensor, including the infrared LED and the red LED

To attach the sensor to a finger as shown in Figure 4.3, a sensor housing was created with a 3D printer (see Figure 4.6). In order to energize the sensor and allow synchronized sensing with the arm position sensors, the PPG sensor is connected to the arm position detection sensor unit.

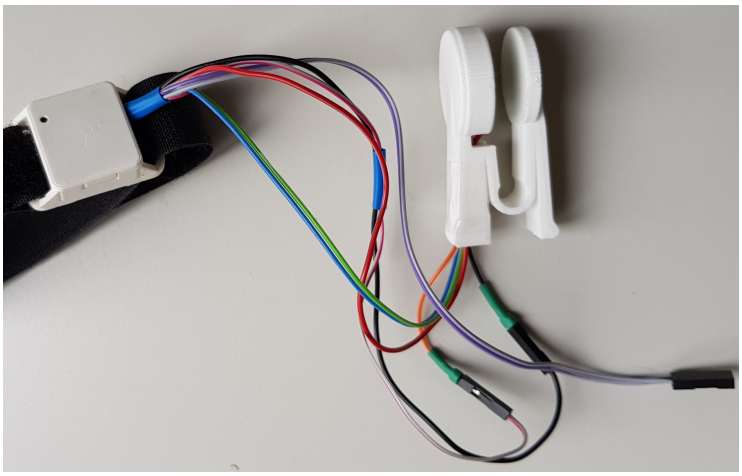

Figure 4.6: **Sensor housings of the PPG sensor and the sensors for arm position detection:** On the right side there is the sensor housing of the PPG sensor and on the left side there is the sensor housing of the sensor unit for arm position detection. The sensors are connected to enable synchronize sensing.

4.1.2 Data Processing

One of the most crucial problems with bio signals is the falsification of these signals by artifacts and noise. Therefore, correction of the signals is necessary in order to guarantee their usability. The goal of correction process is to achieve more accurate results and hence better performance.

ECG Signal

First of all, the DC component has to be canceled [Mah05]. This is achieved by subtracting the average amplitude from each sample of the signal. After canceling the DC component, the signal has to be normalized to one in order to make the depiction intuitively accessible and to be able to later compare it with the PPG, which is also normalized [Mah05].

After normalization, R-peak detection was performed using Biosppy, a Python library for biomedical signal processing. The library applies an algorithm for R-peak detection. This algorithm not only detects the QRS complexes, but also reduces the influence of noise, improving the signal-to-noise ratio [Ham02]. After applying this algorithm, the R-peak detection can be adapted to the filtered signal.

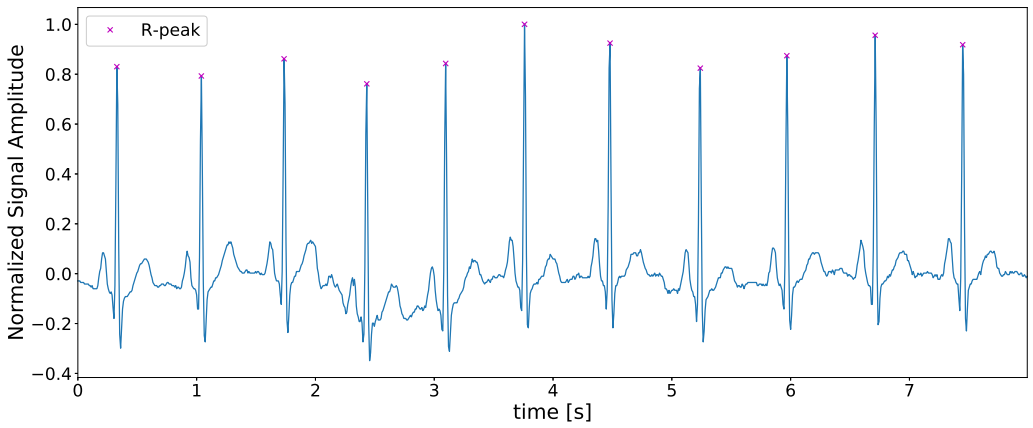

Figure 4.7: **ECG signal:** Section of an ECG signal, which is recorded while the person was at rest. The R-peaks, which represent the first event for PAT calculation, are marked.

PPG Signal

After canceling the DC component of the PPG signal, the signal is normalized, which enables comparing the PPG signal with the ECG signal. For filtering the PPG signal, a fifth order butterworth bandpass filter was applied with a low cut frequency of 0.8 Hz and a high cut frequency of 15 Hz[Car17a].

Subsequently, the point on the PPG signal, which indicates the arrival of the pulse wave, is be determined. As mentioned in Chapter 2, there are different approaches for the description of the point where the pulse wave reaches the distal point. Most of them chose the minimum in one period of the signal as the pulse arrival point [Hol17]. However, Andrew M. Carek et al. provides evidence that the point between the diastolic minimum and inflection point is more accurate [Car17a]. Initially,the PPG signal is windowed between two consecutive R-peaks from the ECG signal. In this window, the diastolic minimum of the PPG signal is determined as the local minimum, whereas the inflection is computed as the maximum of the PPG gradient. For both points, tangents are computed. The point of intersection of the two tangents is the pulse arrival point [Car17a].

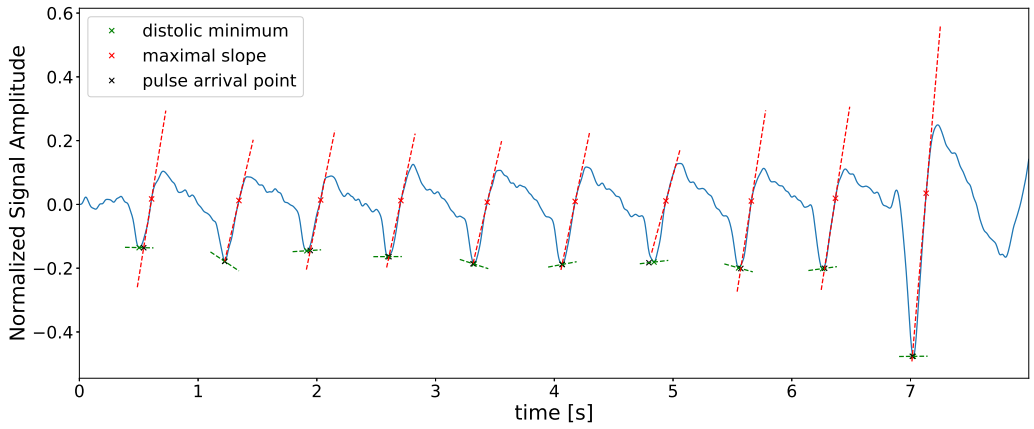

Figure 4.8: **PPG signal:** Section of a filtered PPG signal, which is recorded while the finger was in height of heart. The points where the pulse wave reaches the finger are marked. It is the intersection point of the tangent to the diastolic minimum and the inflection point of a PPG signal.

After obtaining the R-peak of the ECG signal and the pulse arrival point in the PPG signal, the PAT is computed as the time delay between both points as visualized in Figure 4.9.

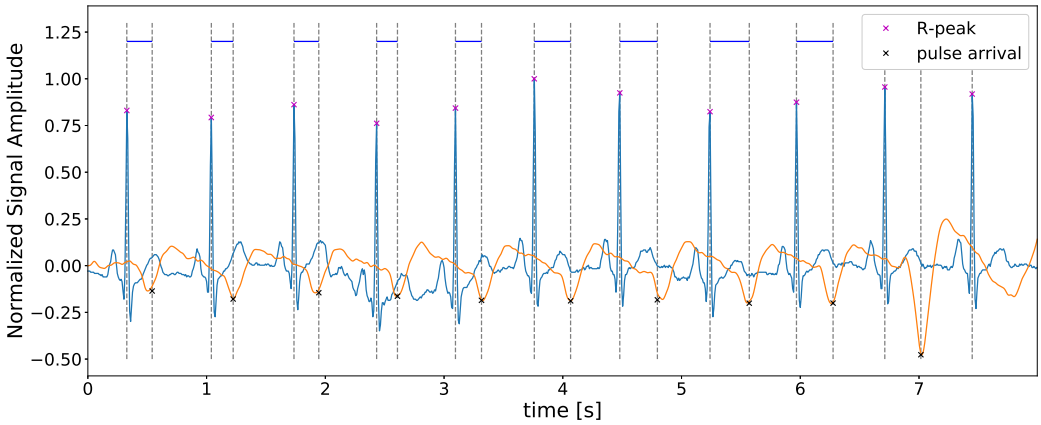

Figure 4.9: **PAT:** Section of an ECG and a PPG signal where the relevant events (R-peaks and pulse arrival points) are mark. The time delay between the R-peaks of the ECG and the pulse arrival point of the PPG is visualized as the interval between two vertical lines.

4.2 Arm Position Detection

The arm position is ascertained with a three-axes accelerometer, a three-axes gyroscope and a barometer, while holding the arm in different positions. A detailed processing structure of the required steps for the detection of the user's arm position is shown in figure 4.10.

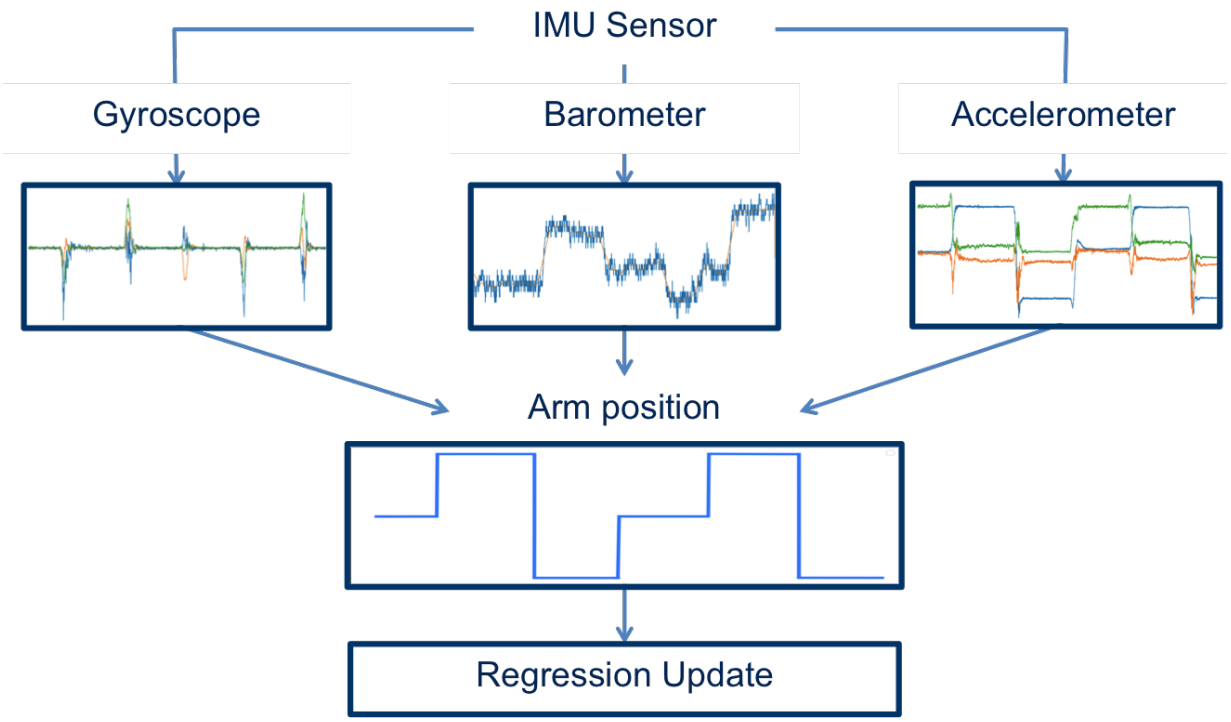

Figure 4.10: **Processing pipeline for arm position detection:** The gyroscope, the barometer and the accelerometer signals are required to calculate the arm position. The arm position then is used to update the regression parameters for blood pressure estimation.

4.2.1 Data Acquisition

The wrist-attached three-axes accelerometer utilized in this thesis enables the detection of three different arm position: arm at height of the heart (hh), arm above the heart (ab), and arm below the heart (bh).

In order to determine whether there is a variation between different arm positions, the system measures not only linear acceleration but also angular velocity using a gyroscope. It is measuring angular velocity. If the object to which the gyroscope is attached to moves, the amplitude's norm of the gyroscope signal increases.

The accelerometer and the gyroscope signal are recorded with the existing IMU BMI160 from Bosch Sensortec. The accelerometer has a range of ± 16 g. The gyroscope of the BMI160 has a range of ± 2000 dps [Bos15].

In addition to the accelerometer and the gyroscope, a barometer is used to determine the user's arm position. This sensor type is used to determine the statistical absolute air pressure. From the absolute atmospheric pressure, the relative height difference of the object to which the sensor is attached can be determined within a certain period of time. Only relative barometer values can be used since the barometer is very sensitive and it is possible that the air pressure values change significantly within a day [Li13]. The barometer returns values in the unit mbar.

This sensor unit is attached to the user's left wrist with a strap. Figure 4.11 shows the orientation of the accelerometer and gyroscope axes. To ensure correct axis alignment, the sensor was always attached to the user's left arm in the same orientation as visualized in Figure 4.12.

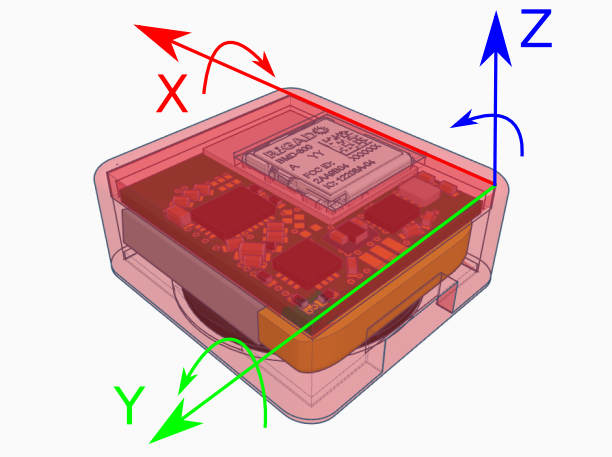

Figure 4.11: **Sensor housing:** The three-axes accelerometer, the three-axes gyroscope and the barometer are integrated in a housing. The axis orientation of the accelerometer and the gyroscope is charted.

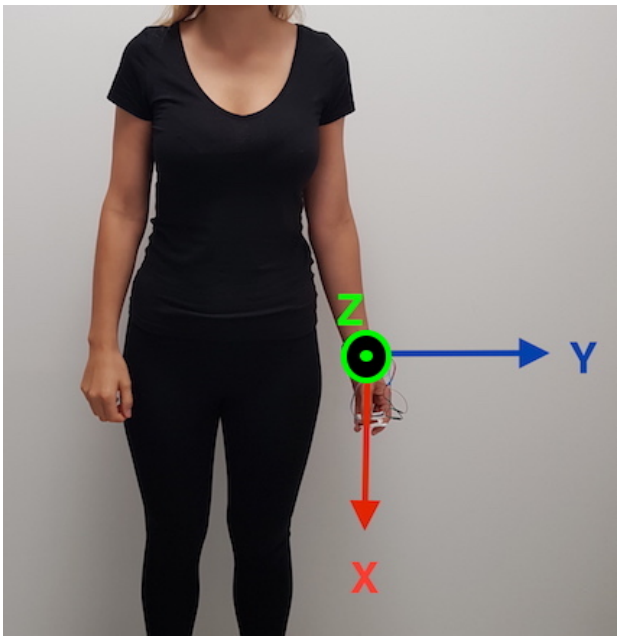

Figure 4.12: **Sensor axes orientation:** The sensor has to be attached to the wrist, so that the axes of the accelerometer and the gyroscope have the shown orientation.

4.2.2 Data Processing

After preprocessing of all signals, the processing pipeline proposed in Figure 4.13 is applied for arm position detection. In this pipeline, general arm movements are detected from gyroscope data. Afterwards, barometer data is used to distinguish between upward and downward arm movements. Finally, the arm position is determined based on accelerometer data.

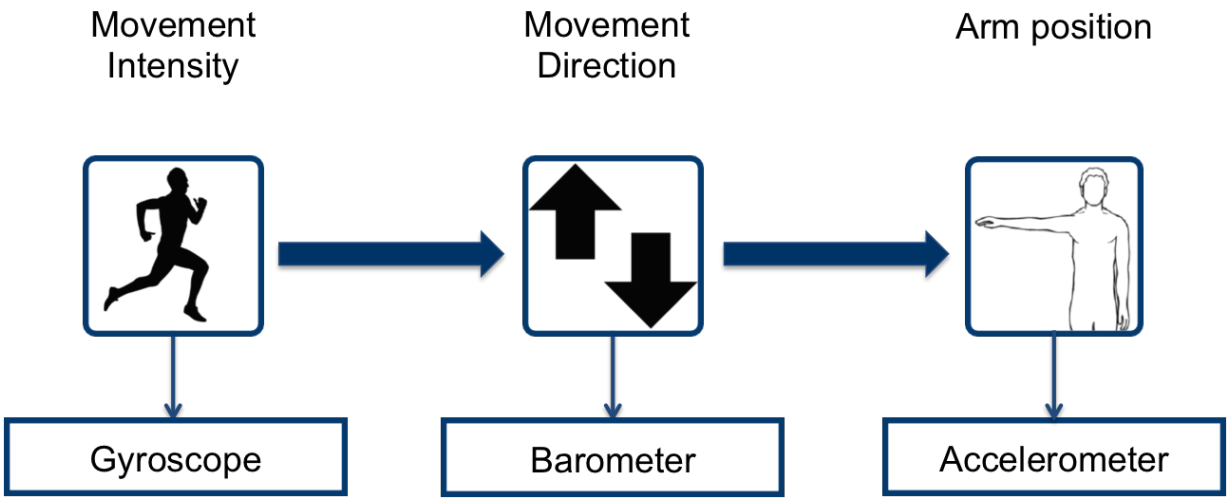

Figure 4.13: **Processing pipeline for arm position detection:** The gyroscope and the barometer data serve the detection of arm position changes, while the accelerometer data serve the actual arm position determination.

Gyroscope

The data sheet of the BMI160 sensor shows that the gyroscope has a scaling factor of 16.4. Each of the three-axes of the sensor is scaled with the respective factors to obtain scaled values. The orientations of the gyroscope axes are shown in Figure 4.11 [Bos15].

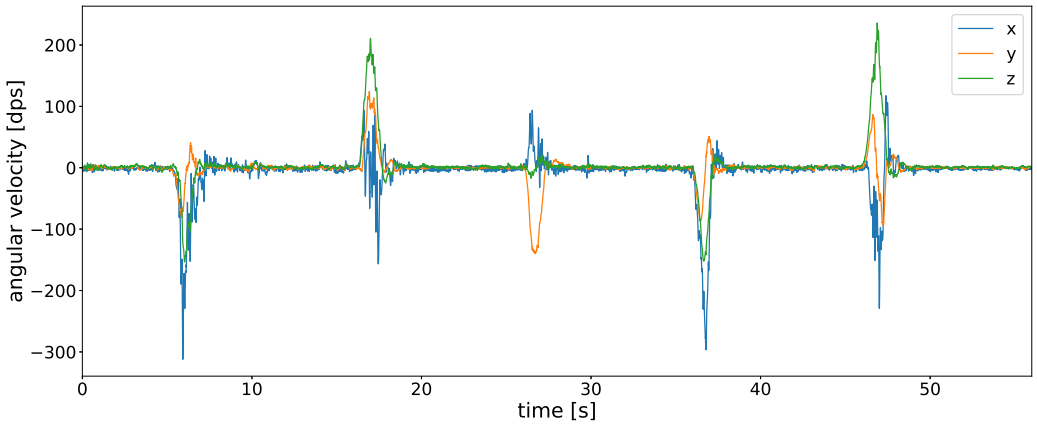

Figure 4.14: **Gyroscope signal:** Three-axes gyroscope signal over a time period of almost one minute. There was a arm position change about every 10 seconds, which produces the rashes of the signals.

As already mentioned, it is not reasonable to measure blood pressure, or an arm position change while a person is moving. For that reason, the movement intensity (MI), which is defined by Zhang et al.[Zha11] as the Euclidean norm over all three gyroscope axes (see Equation 4.1), was used.

$$MI(\mathbf{t}) = \sqrt{g_x^2(t) + g_y^2(t) + g_z^2(t)} \tag{4.1}$$

This feature is independent of the detector's orientation and measures the instantaneous intensity of human motion [Zha11]. For signal smoothing, a first order Butterworth filter with a low cut frequency of 0.1 Hz and a high cut frequency of 0.99 Hz was applied to the computed movement intensity.

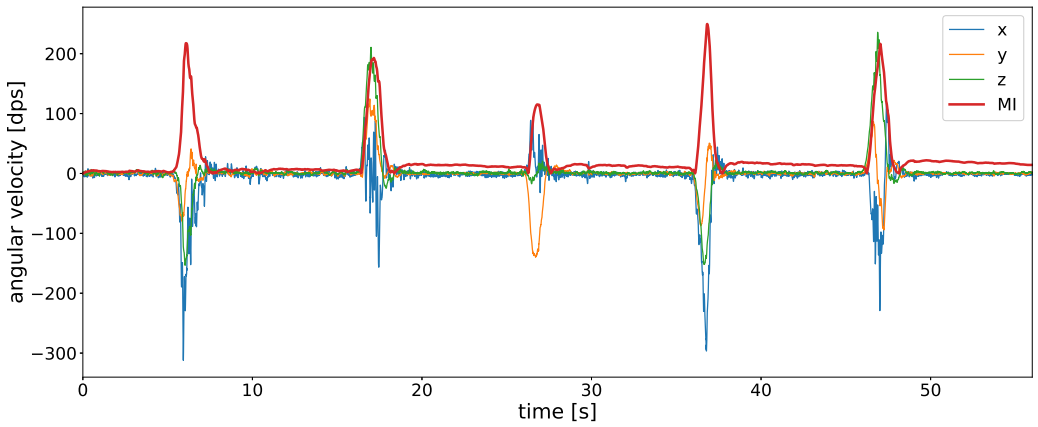

Figure 4.15: **Movement intensity (MI):** Gyroscope signal of the three-axes and the euclidean norm of the three-axes (MI)

A threshold for distinguishing movement from no movement is determined. After considering different test data sets and testing different values, the movement intensity threshold was set to 36 dps.

Barometer

The barometer data is used to determine if a movement detected by the gyroscope actually originated from an arm position change. For signal smoothing, barometer data was filtered with a moving average filter with a window size of 500 samples, which corresponds (see figure 4.16). On the one hand, if the window width is set too low, the filtering has almost no effect on the noisy signal. On the other hand, if the window width is set too large, the signal is extremely smoothed and no usable information can be obtained from the signal data.

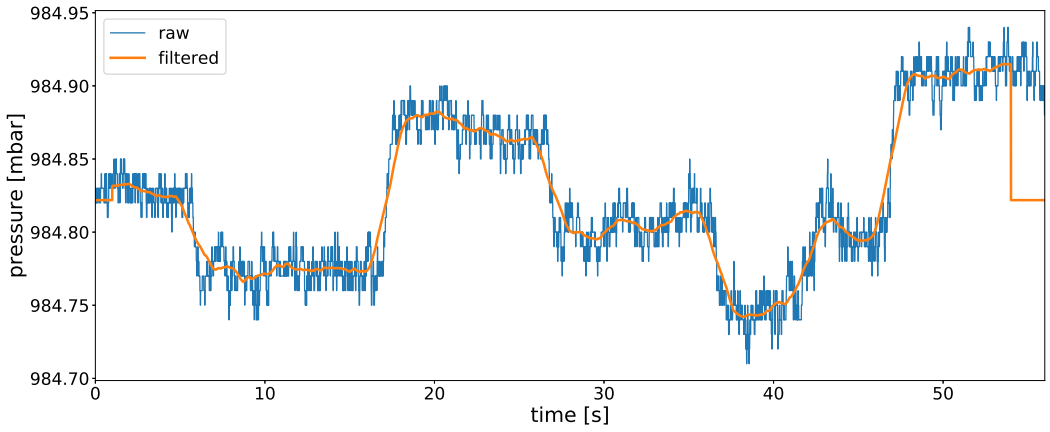

Figure 4.16: **Barometer signal:** The section of a raw barometer signal and of a filtered barometer signal contains increases and decreases due to upward and downward arm movements.

While the gyroscope data is used to determine movement in general, the barometric data is used to determine the type of movement. The barometric signal is normalized to one. The signal is divided into windows with a window size of 250 samples (the sensor's frequency). A threshold was applied for the detection of a position change. The threshold was empirically set to 0.25 of the maximum barometer difference within the window.

To enable the subsequent classification of arm positions, the position change data was set for whole intervals (see Figure 4.17). Since only two different movements can be classified based on the barometric data, the intervals can only be set to two different values. The initial interval is an exception, because all arm positions are possible. After a movement upward the barometer data are set to a certain value and after a movement downward the barometer data is set to another value. In addition to this information, also the previous arm position is taken into account.

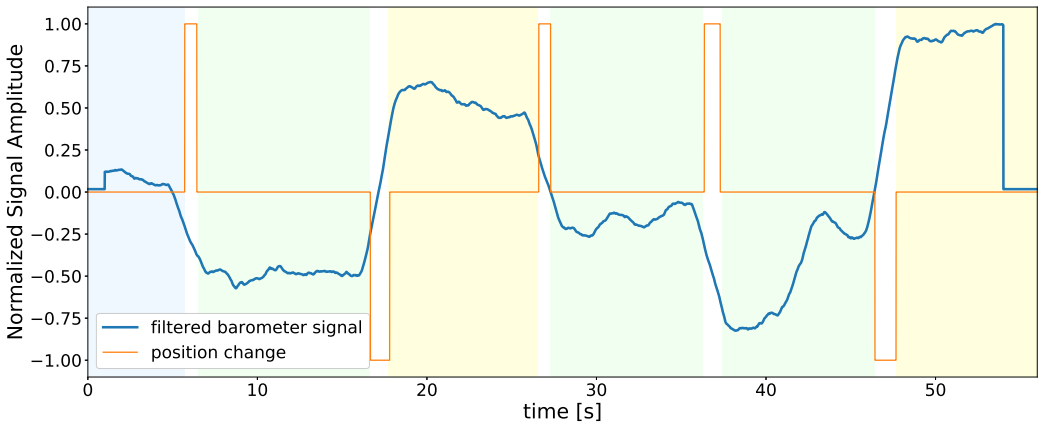

Figure 4.17: **Barometer signal:** After an increase of barometer data one type of arm position can occur after a decrease in barometer data another type of arm position can occur. While the initial interval all arm position are possible.

Accelerometer

The orientation of the accelerometer axes is the same as the orientation of the gyroscope axes, which are shown in Figure 4.11 and Figure 4.12 [Bos15].

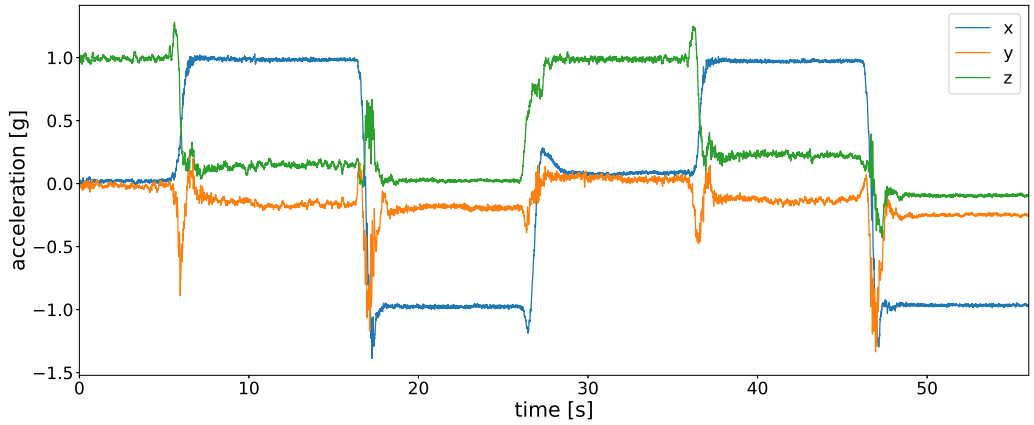

Figure 4.18: **Accelerometer signal:** Raw signal of a three-axes accelerometer, while performing a sequence of six arm positions.

Each arm position has a characteristic value for each of the accelerometer axes. Taking the axes orientation and the attachment of the accelerometer sensor into account, it is possible to determine the different arm positions. As shown in Figure 4.12, it is possible to use the x values directly for classification, since they are unambiguous for each arm positions, while the z and y values are not.

As it is possible to hold the arm in different arm positions or angles of inclination in the different arm heights, the values of the y and z values has to be used in addition to the x values (see Figure 4.19). Based on this data, it is possible to clearly determine the arm position.

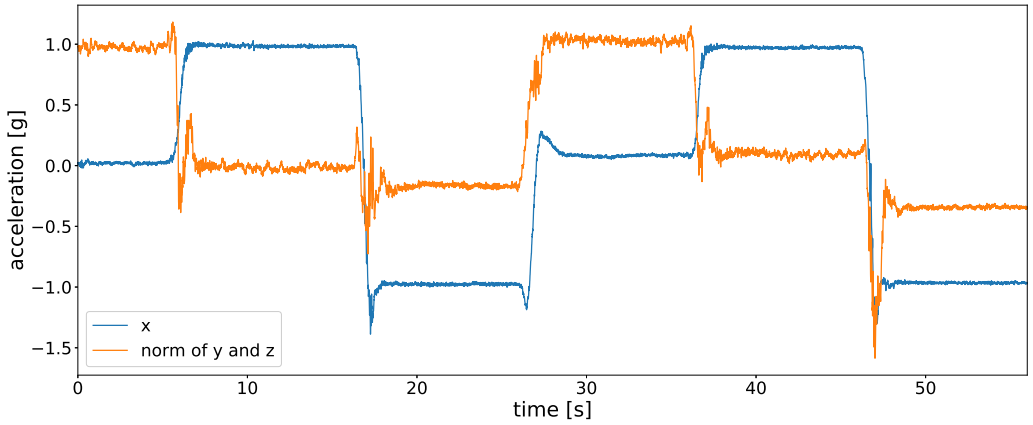

Figure 4.19: **Accelerometer signal:** Signal of the accelerometer's x-axis and the norm of the y- and z-axis, while performing a sequence of six arm positions.

After determining characteristic accelerometer values for every arm position the thresholds between these characteristic values can be calculated. Thereby, the arm position detection algorithm was completed by distinguishing between the different arm positions, based on the accelerometer thresholds. The classification then proceeds as follows: First, the MI, which was acquired from the gyroscope, is queried. If the value is lower than 36 dps, there is no movement and it is possible to determine the arm position.

Considering the fact that no arm position change has happened before the initial arm position interval, the barometer data cannot be included for the first arm position interval. Therefore, the next step is to analyze the accelerometer data and categorize the data into the corresponding areas, which were defined by the means of the calculated thresholds.

However, after changing arm position for the first time it is possible to determine the arm position of the person who is wearing the sensor system, by incorporating the barometric information in the calculations.

Chapter 5

Evaluation

This section describes the study design regarding the evaluation of the developed arm position detection method. The arm position detection was intended to be used for reducing hydrostatic errors in blood pressure estimation. Unfortunately, technical problems with the ECG sensor occurred so that is was not possible to obtain reliable PAT measurements. Nonetheless, the developed and presented method for arm position detection is operational on its and can be evaluated as a stand-alone system.

5.1 Study Design

Since the PPG signal was acquired from the user's finger, the PAT depends on the user's arm position. Therefore, different arm heights relative to the heart can influence the PAT due to changes in hydrostatic pressure. If the sensor is above the heart, the PAT increases and therefore, the blood pressure estimation suggests a decrease in blood pressure. If the sensor is below the heart, the PAT decreases and naturally, the BP is increased. Since the estimated BP does not correspond to the actual BP, the PAT has to be adjusted by the user's arm position.

PAT calculations have to be corrected by several parameters. Therefore, three different arm positions were considered: arm in height of heart (hh), arm above heart (ah) and arm below heart (bh). Additionally, the three different the arm positions were combined with three different body postures: standing, sitting and lying. Figures 5.1 - 5.3 illustrate the three body postures, each with the three described arm positions.

A reliable blood pressure measurement is only possible when the body is at rest [Li08]. If the person moves, it is possible that arm positions may change rapidly and the measured PAT is not stable.

Figure 5.1: **Standing body posture:** Subject performing the three defined arm positions (hh, ah and bh) while standing.

Figure 5.2: **Sitting body posture:** Subject performing the three defined arm positions (hh, ah and bh) while sitting.

Figure 5.3: **Lying body posture:** Subject performing the three defined arm positions (hh, ah and bh) while lying.

5.2 Data collection

For the evaluation of the developed arm position detection method, data of 15 healthy test persons was collected. The subjects did not need to meet any requirements, except healthiness and that they feel able to complete the study. All probands signed a written informed consent form before participating in the study. Additional anthropometric characteristics of the participants are shown in Table 5.1.

Table 5.1: **Study probands' characteristics:** Anthropometric characteristics of the 15 participants of the study

Gender	Age in years	Height in cm	Weight in kg
9 male, 6 female	23.3 ± 2.7	178 ± 19	73.2 ± 18.8

After attaching the sensor unit to the left arm, every subject had to hold the arm in a randomly defined sequence of arm positions. For each body posture, three data sets of different arm positions were recorded. Each record consists of a sequence of six arm positions as each of the three arm positions occur exactly twice. In addition, each sequence began with another arm positions.

An example sequence for a randomly selected subject and posture is provided in Table 5.2. The following information and data are from a randomly chosen study participant. The table and the associated graphs refer to the standing body posture. Each arm position was held for approximately ten seconds, so that every sequence has a total length of one minute.

Table 5.2: **Study procedure example:** Study procedure with three arm position sequences for one participant and one of three body postures (hh = heart height, ah = above heart, bh = below heart)

Arm position	1	2	3	4	5	6
Sequence 1	hh	ah	bh	hh	ah	bh
Sequence 2	ah	bh	ah	bh	hh	hh
Sequence 3	bh	hh	ah	hh	bh	ah

Chapter 6

Results

This section presents the evaluation results of the developed arm position detection method. The section is divided into two subsections: The first subsection presents the measurement results and the second subsection presents the performance concerning the accuracy of the arm position detection.

6.1 Measurements

For reasons of illustration, Figure 6.1 showcase recordings of gyroscope, barometer, and accelerometer signals for the three sequences of arm positions described in Table 5.2. For presentation purposes, the signals for each sensor were normalized.

In order to determine which values are based on which arm position, the mean and median values of the recorded arm positions were calculated. In total, arm position sequences of the first 5 participants were calculated for each of the three body postures. It was observed that the results of the standing recordings only slightly differed compared to recordings while subjects were sitting. Therefore, the same thresholds and decision rules for arm position detection were used for both postures. Tables 6.1 and 6.2 show resulting mean and median values, respectively. In the first line of the tables, the form accelerometer "axis, arm position" indicates from which arm position the values below originate.

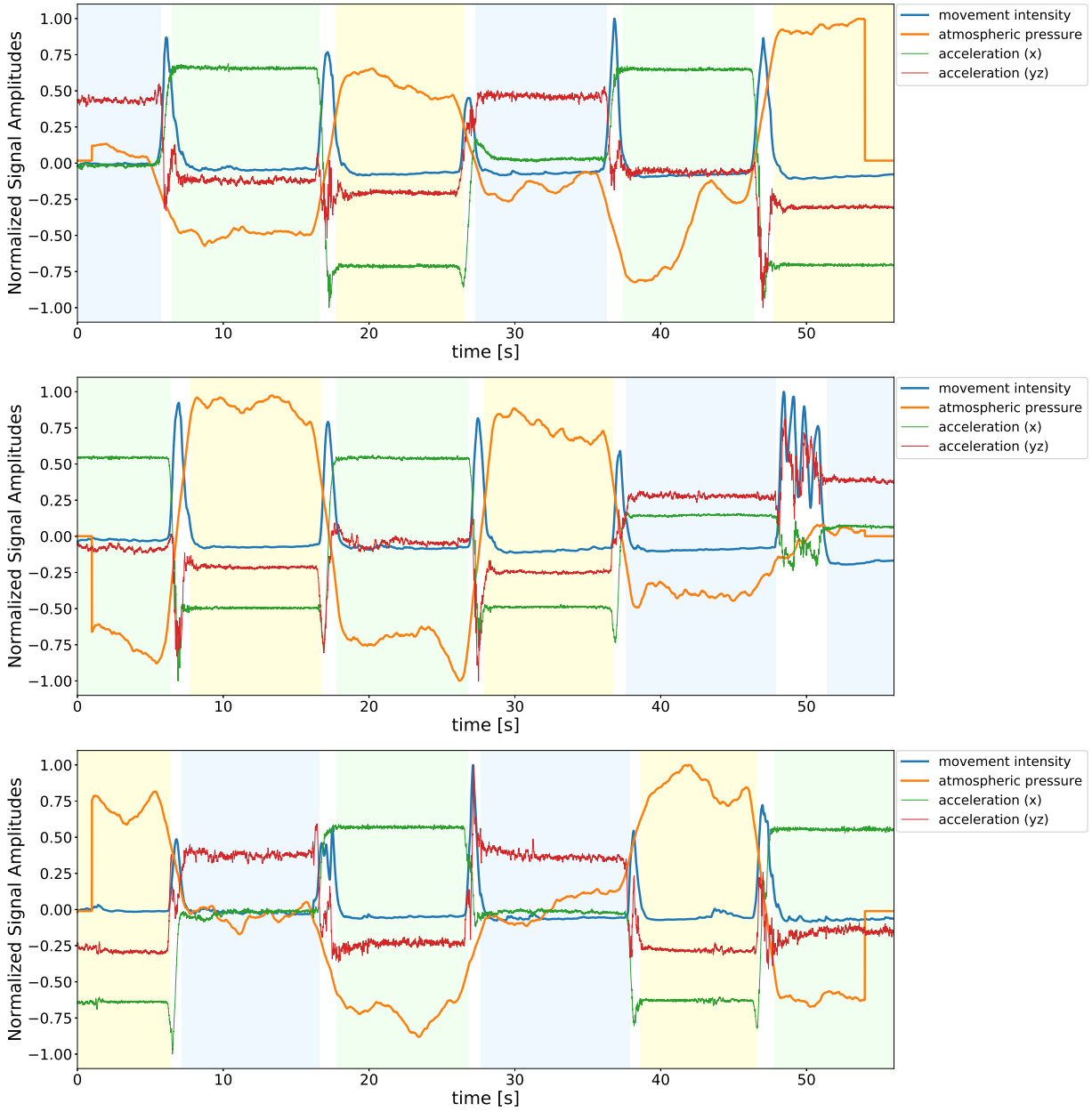

Figure 6.1: **Arm position sequences:** Movement intensity, barometer, and accelerometer signal of the arm position sequences of Table 5.2. The different arm positions are marked in different colors (blue = hh, green = ah, yellow = bh).

Table 6.1: **Mean and median for the standing and sitting body posture:** Mean and median values of the accelerometer signal, while probands were standing or sitting.

axis, arm position:	**x, hh**	**x, ah**	**x, bh**	**yz, hh**	**yz, ah**	**yz, bh**
mean in g	-0.1036	0.8644	-0.8686	0.8119	0.0152	-0.1993
median in g	-0.1045	0.8655	-0.8654	0.8081	0.0102	-0.2015

Table 6.2: **Mean and median for the lying body posture:** Characteristic mean and median values of the accelerometer signal, while the probands were lying.

axis, arm position:	**hh-x**	**ah-x**	**bh-x**	**hh-yz**	**ah-yz**	**bh-yz**
mean in g	-0.0633	0.7035	-0.5243	-0.3089	0.0289	-0.5189
median in g	-0.0637	0.7052	-0.5661	-0.3091	0.0263	-0.5478

After the mean and median values were calculated, it was possible to determine the thresholds that mark the boundary between the different arm positions. In the case of the x-values, it was possible to make a clear distinction between the arm positions hh, ah and bh. Therefore, a threshold was created between hh - ah and hh - bh. In order to do so, the exact value between the two calculated mean/median values were used. For the yz values, the thresholding was more difficult. In the standing and sitting body postures, the arm positions ah and bh were combined due to their similarity (in arm angulation). In the body posture lying, the arm positions bh and hh were combined. After that, the threshold could be formed between hh - ah / bh (Standing/Sitting) and between ah - bh / hh (Lying).

Tables 6.3 and 6.4 show the thresholds based on median and mean are almost similar. Therefore, the mean-based threshold was used for later evaluation. With these thresholds it is possible to divide the accelerometer data into different areas, enabling the classification of various arm positions.

Table 6.3: **Thresholds for standing and sitting body postures:** Accelerometer boundaries between different arm positions while the probands are standing or sitting

axis, arm position	**x, hh-ah**	**x, hh-bh**	**yz, hh-ah/bh**
mean in g	0.3804	−0.4861	0.3600
median in g	0.3805	−0.4850	0.3562

Table 6.4: **Thresholds for the lying body posture:** Accelerometer boundaries between different arm positions while the probands are lying

axis, arm position	**x, hh-ah**	**x, hh-bh**	**yz, ah-hh/bh**
mean in g	0.3201	−0.2938	−0.1925
median in g	0.3207	−0.3149	−0.2011

After determining these thresholds, the arm position detection algorithm was completed by distinguishing between the different arm positions, based on the accelerometer thresholds. The classification then proceeds as described in Chapter 4.

6.2 Performance

The performance of the developed method for arm position detection is presented using a confusion matrix. The rows of the confusion matrix represent the performed arm positions, while the columns represent the predicted arm positions. To get a better idea of the meaning of these values, the following calculations are presented for a binary classification problem (see Table 6.5 and Equations 6.1 - 6.4) [Lar13].

Table 6.5: **Classification scores:** Overview of the classification scores

Name	Abbreviation	Description
True Positive	**TP**	Number of positive instances that were classified as positive
True Negative	**TN**	Number of negative instances that were classified as negative
False Positive	**FP**	Number of negative instances that were classified as positive
False Negative	**FN**	Number of positive instances that were classified as negative

Accuracy

The accuracy is the standard metric to summarize the general classification performance for all classes and measures the percentage of correct identifications after discounting insertion, deletion, and substitution errors [Faw06]. Accuracy is defined as

$$accuracy = \frac{TP + TN}{TP + TN + FP + FN} \quad . \tag{6.1}$$

Precision

Precision, which is also referred to the PPV (positive predictive value), measures the probability that a detected arm position corresponds to an actual arm position [Faw06]. Precision is defined as

$$precision = \frac{TP}{TP + FP} \quad . \tag{6.2}$$

Recall

The recall, also known as sensitivity, corresponds to the correct detection rate relative to ground truth. It can be equated with the percentage of correctly recognized events of all true instances of a particular class, averaged over all events [Faw06]. Recall is defined as

$$recall = \frac{TP}{TP + FN} \quad . \tag{6.3}$$

F1-Score

The F1-Score combines the precision and recall rates into a single measure of performance [Faw06]. F1-Score is defined as

$$F1 = \frac{2 * precision * recall}{precision + recall} \quad . \tag{6.4}$$

Although these metrics are defined for binary classification, they can be generalized for a multi-class problem leading to a one-against-all classification. Therefore, an instance can be positive or negative with respect to a particular class, e.g., only instances of arm position hh would be considered as positive whereas instances of all other arm positions would be considered as negative [Lar13].

For the arm position detection, an overall accuracy of 94.44 % was achieved. The confusion matrix (see Figure 6.2) and Table 6.6 show the classification results for all three body postures.

For further analysis and to discuss potential systematic errors, the results were divided into the different body postures.

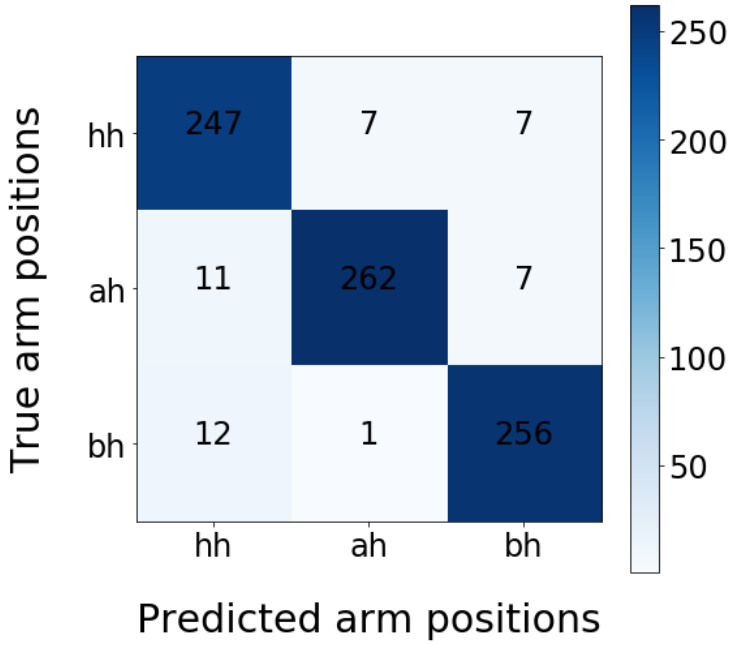

Figure 6.2: **Total confusion matrix:** The confusion matrix shows the classification results for all body postures. The scale to the right of the matrix shows the color assignment for the frequency of occurrence.

Table 6.6: Overview of the metrics for the total confusion matrix

	Precision	**Recall**	**F1-Score**
Arm position hh	91.48 %	94.64 %	93.03 %
Arm position ah	97.04 %	93.57 %	95.27 %
Arm position bh	94.81 %	95.17 %	94.99 %
Total	94.51 % $\pm$ 3.03 %	94.44 % $\pm$ 0.87 %	94.46 % $\pm$ 1.43 %

Standing

In this body posture, the accuracy amounts to 96.30 %. For the body posture standing, the classification results are listed in the confusion matrix (see Figure 6.3) and in Table 6.7. While the subjects were standing, almost no misclassifications occurred.

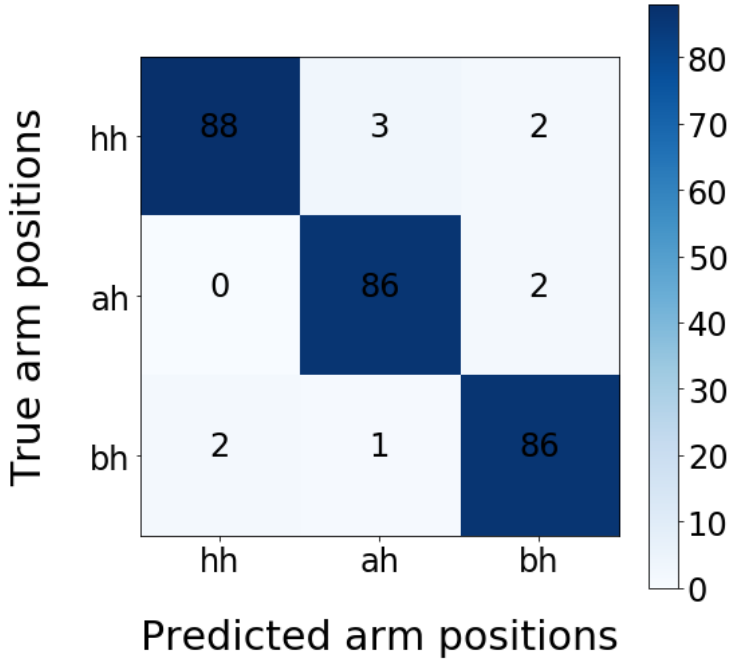

Figure 6.3: **Standing confusion matrix:** The confusion matrix shows the classification results for the body posture standing. The scale to the right of the matrix shows the color assignment for the frequency of occurrence.

Table 6.7: Overview of the metrics for the confusion matrix of the standing body posture

	Precision	**Recall**	**F1-Score**
Arm position hh	97.78 %	94.62 %	96.17 %
Arm position ah	95.56 %	97.73 %	96.63 %
Arm position bh	95.56 %	96.63 %	96.09 %
Total	96.32 % ± 1.46 %	96.30 % ± 1.68 %	96.29 % ± 0.34 %

Sitting

An accuracy of 95.93 % was achieved while the subjects were sitting. The classification results for the body posture sitting can be extracted from the confusion matrix (see Figure 6.4) and Table 6.8. An overall number of 11 misclassifications occurred. Between the arm positions hh and ah, more frequent erroneous assignments happened.

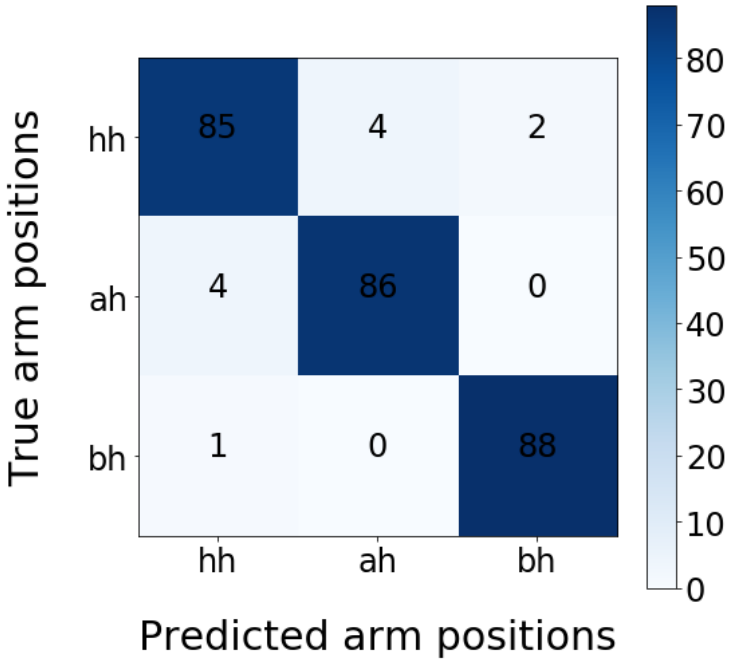

Figure 6.4: **Sitting confusion matrix:** The confusion matrix shows the classification results for the body posture sitting. The scale to the right of the matrix shows the color assignment for the frequency of occurrence.

Table 6.8: Overview of the metrics for the confusion matrix of the sitting body posture

	Precision	**Recall**	**F1-Score**
Arm position hh	94.44 %	93.41 %	93.92 %
Arm position ah	95.56 %	95.56 %	95.56 %
Arm position bh	97.78 %	98.88 %	98.32 %
Total	95.91 % ± 1.87 %	95.93 % ± 2.95 %	95.92 % ± 2.40 %

Lying

The lowest accuracy 91.11 % was achieved while the patients were lying. The confusion matrix (see Figure 6.5) and Table 6.9 show the classification results for the body postures lying. While all predicted arm positions with the sensors above the heart were detected correctly, the other predicted arm position were misclassified more frequently.

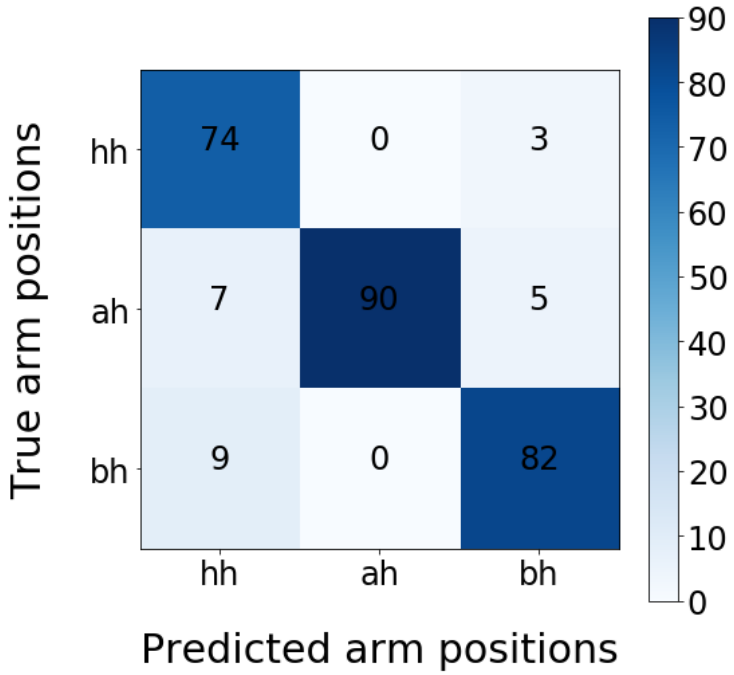

Figure 6.5: **Lying confusion matrix:** The confusion matrix shows the classification results for the body posture lying. The scale to the right of the matrix shows the color assignment for the frequency of occurrence.

Table 6.9: Overview of the metrics for the confusion matrix of the lying body posture

	Precision	**Recall**	**F1-Score**
Arm position hh	82.22 %	96.10 %	88.62 %
Arm position ah	100.00 %	88.24 %	93.75 %
Arm position bh	91.11,%	90.11 %	90.61 %
Total	91.93 % ± 9.71 %	91.11 % ± 2.87 %	91.23 % ± 2.61 %

Chapter 7

Discussion

7.1 Arm Position Detection

The presented results provide evidence that the presented method for arm position detection is functioning. The overall accuracy of 94.44 % shows that the classification of different arm positions was possible with the proposed approach. As apparent from the study results in the body posture standing the highest accuracy of 96.30 % were achieved. Additionally there were hardly misclassification while the probands were standing. Simulating a total of 270 arm positions, only 10 were assigned to a wrong arm position. The associated confusion matrix show that these misclassifications when standing were balanced. Such a high accuracy was achieved due to the fact, that the freedom of movement of the subjects was not limited in any way. During the recording they stand freely in the room and no subject restricted the subjects.

While the probands were sitting an approximate accuracy of 95.93 % were achieved. Even while sitting, there hardly were misclassifications. An overall number of 11 misclassifications occurred. The misclassifications in sitting body postures were not that evenly distributed than while standing. In that case, the confusion matrix show that the misclassifications when frequently occurred between the arm positions hh and ah. This phenomenon might have occurred by chance. Another potential explanation is, that while sitting it was more difficult for the test persons to estimate when the arm was over the heart and when it was under the heart. For instance, if a subject was instructed to hold his arm heart height, and the subject held his arm up at a certain angle, the algorithm falsely recognized that arm position hh as ah. This problem can be safely ignored as it did not occur frequently. Additionally, this problem can be neglected, since the misallocation, according to the just presented explanation attempt, does not necessarily entail incorrect results.

However, results ere slightly worse for the lying body posture. In this case, there are more misclassifications. In particular, false positives were detected if subjects were instructed to hold their arms at heart height. One possible explanation is that signals for the arm positions bh and hh showed a large similarity among some subjects. This phenomenon is dependent on the physical capabilities of the subject. For some subjects, the range of motion of the shoulder (and thus of the arm) was considerably limited. They were unable to let their arms hang down at a high angle. For obvious reasons, it rarely occurs that while someone is lying the arm is held below the heart. However, an arm position below heart height while lying rarely occurs during daily-life circumstances. Therefore, it might be reasonable to distinguish only between two arm positions by combining the two arm positions that were confused with each other into one defined arm position. This suggestion is supported by the fact, that the detection of arm position ah showed an accuracy of 100 %.

This study is limited by the fact that the data collection for the evaluation of the arm position detection method was conducted under laboratory conditions. Therefore, the specified arm and body positions were only considered in a state of immobility. Future work should therefore verify the functionality of the presented method during everyday activities.

7.2 Blood Pressure Estimation

An algorithm for PAT calculation based on an ECG and a PPG signal is presented in Chapter 4. This algorithm was developed using a single record over a time of 25 second. Based on this record no insightful results can be provided. Unfortunately, it was not possible to record more data due to problems with the ECG sensor. Since the algorithm for PAT calculation wasn't evaluated, no blood pressure values can be estimated. Moreover, the arm position detection in combination with the PAT calculation could not be evaluated either. The intention was to record ECG and PPG signals for different arm positions and calculate the average PAT for each arm position. After data has been collected, the equation's coefficients (see Equation 3.1) for blood pressure estimation have to be adjusted. If the sensors, algorithms and calculations are functional, it is possible to represent the calculated PAT and BP values by means of a linear regression. Nevertheless, the existing PAT calculation algorithm establish a basis for an unobtrusive blood pressure estimation.

Chapter 8

Conclusion and Outlook

This thesis provides the basis for the development of a unobtrusive blood pressure monitoring. Therefore, the pulse arrival time between ECG R-peak and PPG pulse wave onsets was computed and a linear regression was applied for estimating the blood pressure. The ECG signal was acquired by a ECG sensor, which is attached to the chest. A PPG sensor, whereas the PPG signal was acquired from the left index finger. Based on recorded data from these sensors, an algorithm for pulse arrival time calculation is presented in this thesis.

The PPG signal is affected by the hydrostatic pressure, which is dependent on the user's arm position due to the influence of gravity. Therefore, the main purpose if this thesis was the development of a method for arm position detection, in order to eliminate the effects of hydrostatic pressure. This method was implemented by a sensor unit and the development of an algorithm that provides precise information concerning a user's arm position relative to the heart. The wrist-worn sensor system included a accelerometer, gyroscope and barometer. Three arm positions were considered: Arm above heart, below heart and at heart height. The feasibility of the proposed method and algorithm was evaluated on 15 healthy test persons.

The evaluation of the arm position detection showed that the presented solution is capable of correctly detecting the user's arm position. The arm position classification showed an overall accuracy of 94.44 %, a precision of 94.51 %, a recall of 94.44 %, and a F1-score of 94.46 %. Irrespective of whether the test persons were standing, sitting or lying, the algorithm achieved performance parameters beyond 90 percent. In conclusion, the presented results demonstrated the capability of the developed method to detect users' arm positions. Thus, it provides the basis to eliminate the effects of hydrostatic pressure in order to obtain reliable blood pressure values.

However, further research needs to be done in order to finalize a device for unobtrusive blood pressure measurement involving the developed method. At first, the functionality of the developed

method should be tested on a larger scale as well as during everyday activities. Further available data might help to create an even more robust arm position detection algorithm. In a second step, the arm position detection should be used to eliminate the hydrostatic error, in order to determine correct pulse arrival time and thus, blood pressure values. Finally, a convenient and unobtrusive device containing all necessary sensors should be designed and tested for its usability during the daily life activities.

Appendix A

Patents

Body-worn system for measureing continuous non-invasive blood pressure (cNIBP)

Pub. No.	US 2010/0160794 A1
Pub. Date	Jun. 24, 2010
Inventors	Matt, Banet; Marshal, Dhillon; McCombie, Devin B.

Abstract

The present invention provides a technique for continuous measurement of blood pressure based on pulse transit time and which does not require any external calibration. This technique, referred to herein as the Composite Method, is carried out with a body-worn monitor that measures blood pressure and other vital signs, and wirelessly transmits them to a remote monitor. A network of body-worn sensors, typically placed on the patient's right arm and chest, connect to the body-worn monitor and measure time-dependent ECG, PPG, accelerometer, and pressure waveforms. The disposable sensors can include a cuff that features an inflatable bladder coupled to a pressure sensor, three or more electrical sensors (e.g. electrodes), three or more accelerometers, a temperature sensor, and an optical sensor (e.g., a light source and photodiode) attached to the patient's thumb.

Apparatus and method for measuring blood pressure

Pub. No.	US 2008/0214942 A1
Pub. Date	Sep. 4, 2008
Inventors	Oh, Hyun-Ho; Shim, Bong-Chu; Kim, Gyoung-Soo; Ku, Yun-Hee; Cho, Seong-Moon; Hong, Hyung-Ki; James Hill; Yves Schutz

Abstract

Disclosed are an apparatus and method for measuring a blood pressure capable of enhancing accuracy and reliability for a blood pressure. According to the apparatus and method, a blood pressure is obtained by using a pulse transit time (PTT) calculated based on a pulse wave measured with a minimized error, a subject's body information, pulse analysis information, and environment information together measured when measuring the pulse wave.

Calibration of Pulse Transit Time Measurements to Arterial Blood Pressure using External Arterial Pressure Applied along the Pulse Transit Path

Pub. No.	US 2010/0241011 A1
Pub. Date	Sep. 23, 2010
Inventors	McCombie, Devin B.; Asada, Haruhiko H.; Reisner, Andrew

Abstract

An apparatus and methods for adaptive and autonomous cali bration of pulse transit time measurements to obtain arterial blood pressure using arterial pressure variation. The appara tus and methods give pulse transit time (PTT) devices an ability to self-calibrate. The methods apply a distributed model with lumped parameters, and may be implemented, for example, using pulse transit time measurements derived from a wearable photoplethysmograph (PPG) sensor architecture with an intervening pressurizing mechanism.

Wearable pulse wave velocity blood pressure sensor and methods of calibration thereof

Pub. No.	US 7,674.231 B2
Pub. Date	Mar. 9, 2010
Inventors	McCombie, Devin B.; Reisner, Andrew T.; Asada, Haruhiko H.; Shaltis, Phillip

Abstract

An apparatus and methods for performing a circulatory measurement on an extremity, such as a hand, of a subject. The circulatory measurement results in the derivation of an output circulatory metric that may encompass blood pressure or various other circulatory metrics. An indicator of an input circulatory metric at a locus on the extremity is measured, Such as a pulse transit time, and calibrated to account for the hydrostatic component of blood pressure arising due to Ver tical displacement of the extremity with respect to the heart.

Wearable blood pressure sensor and method of calibration

Pub. No.	US US 7,641,614 B2
Pub. Date	Jan. 5, 2010
Inventors	Asada, Haruhiko H.; Shaltis, Phillip; McCombie, Devin B.; Reisner, Andrew T.

Abstract

Methods and apparatus for measuring arterial blood pressure at an extremity of a subject. Arterial blood pressure is derived from a circulatory measurement performed on an extremity of a Subject and the circulatory measurement is normalized to account for the instantaneous vertical displacement of the extremity. The vertical displacement of the extremity relative to the heart of the Subject is obtained using the angular ori entation of the subjects extremity. An improved photopl ethysmograph can discriminate light traversing the extremity from ambient light on the basis of differential response. The apparatus may have a conducting polymer actuator for apply ing pressure to the extremity of the Subject. A pulsatile wave form from the photoplethysmographic signal may be obtained at a plurality of externally applied pressures to cali brate the photoplethysmograph.

List of Figures

List of Tables

Bibliography

[Bon10] P. Bonato: *Wearable sensors and systems*, *IEEE Engineering in Medicine and Biology Magazine*, Bd. 29, Nr. 3, 2010, S. 25–36.

[Boo77] J. Booth: *A Short History of Blood Pressure Measurement*, *Proceedings of the Royal Society of Medicine*, Bd. 70, Nr. November, 1977, S. 793–799.

[Bos15] Bosch Sensortec: *BMI160 Small, low power inertial measurement unit*, *www.Bosch-Sensortec.Com*, 2015.

[Bux15] D. Buxi, J.-M. Redouté, M. R. Yuce: *A survey on signals and systems in ambulatory blood pressure monitoring using pulse transit time*, *Physiological Measurement*, Bd. 36, Nr. 3, 2015, S. R1–R26.

[Car17a] A. M. Carek, J. Conant, A. Joshi, H. Kang, O. T. Inan: *SeismoWatch*, *Proceedings of the ACM on Interactive, Mobile, Wearable and Ubiquitous Technologies*, Bd. 1, Nr. 3, 2017, S. 1–16.

[Car17b] A. M. Carek, J. Conant, A. Joshi, H. Kang, O. T. Inan: *SeismoWatch: Wearable Cuffless Blood Pressure Monitoring Using Pulse Transit Time*, *Proceedings of the ACM on Interactive, Mobile, Wearable and Ubiquitous Technologies*, Bd. 1, Nr. 3, 2017, S. 1–16.

[Che13] H. M. Cheng, D. Lang, C. Tufanaru, A. Pearson: *Measurement accuracy of non-invasively obtained central blood pressure by applanation tonometry: A systematic review and meta-analysis*, *International Journal of Cardiology*, Bd. 167, Nr. 5, 2013, S. 1867–1876.

[Chu13] E. Chung, G. Chen, B. Alexander, M. Cannesson: *Non-invasive continuous blood pressure monitoring: a review of current applications*, *Frontiers of Medicine*, Bd. 7, Nr. 1, 2013, S. 91–101.

[Din16] X. R. Ding, N. Zhao, G. Z. Yang, R. I. Pettigrew, B. Lo, F. Miao, Y. Li, J. Liu, Y. T. Zhang: *Continuous Blood Pressure Measurement From Invasive to Unobtrusive: Celebration of 200th Birth Anniversary of Carl Ludwig*, *IEEE Journal of Biomedical and Health Informatics*, Bd. 20, Nr. 6, 2016, S. 1455–1465.

[Drz83] G. M. Drzewiecki, J. Melbin, A. Noordergraaf: *Arterial tonometry: Review and analysis*, *Journal of Biomechanics*, Bd. 16, Nr. 2, 1983, S. 141–152.

[Faw06] T. Fawcett: *An introduction to ROC analysis*, *Pattern Recognition Letters*, Bd. 27, Nr. 8, 2006, S. 861–874.

[Ged81] L. A. Geddes, M. H. Voelz, C. F. Babbs, J. D. Bourland, W. A. Tacker: *Pulse Transit Time as an Indicator of Arterial Blood Pressure*, *Psychophysiology*, Bd. 18, Nr. 1, 1981, S. 71–74.

[Ges12] H. Gesche, D. Grosskurth, G. Küchler, A. Patzak: *Continuous blood pressure measurement by using the pulse transit time: Comparison to a cuff-based method*, *European Journal of Applied Physiology*, Bd. 112, Nr. 1, 2012, S. 309–315.

[Gol99] M. J. Golden: *Clamp arm position sensing apparatus*, 1999.

[Hae05] C. A. Haensch, J. Jörg: *Evaluation of Blood Pressure Regulation in Autonomic Dysfunction*, *Klinische Neurophysiologie*, Bd. 36, Nr. 2, 2005, S. 86–97.

[Ham02] P. Hamilton: *Open source ECG analysis*, *Computers in Cardiology*, 2002, S. 101–104.

[Har10] M. U. Haruhiko H. Asada, Lincoln, MA (US) Philip Shaltis, Newton, M. Devin B. McCombie, Medford, MA (US); Andrew T. Reisner, Newton, (US): *Wearable Blood Pressure Sensor and Method of Calibration*, 2010.

[He14] X. He, R. A. Goubran, X. P. Liu: *Secondary peak detection of PPG signal for continuous cuffless arterial blood pressure measurement*, *IEEE Transactions on Instrumentation and Measurement*, Bd. 63, Nr. 6, 2014, S. 1431–1439.

[Hol17] C. Holz, E. J. Wang: *Glabella: Continuously Sensing Blood Pressure Behavior using an Unobtrusive Wearable Device*, *Proceedings of the ACM on Interactive, Mobile, Wearable and Ubiquitous Technologies*, Bd. 1, Nr. 3, 2017, S. 1–23.

[Kor05] N. Kortokoff: *On methods of studying blood pressure*, *Izv. Venno-Med. Akad.*, Bd. 11, 1905, S. 365.

[Lan07] F. Lang, P. Lang: *Basiswissen Physiologie*, Springer Medizin Verlag, Heidelberg, 2. auflage. Ausg., 2007.

[Lar13] O. D. Lara, M. A. Labrador: *A Survey on Human Activity Recognition using Wearable Sensors*, *IEEE Communications Surveys & Tutorials*, Bd. 15, Nr. 3, 2013, S. 1192–1209.

[Li08] Q. Li, J. A. Stankovic, M. Hanson, A. Barth, J. Lach: *Accurate, Fast Fall Detection Using Posture and Context Information*, *Sensys'08: Proceedings of the 6th Acm Conference on Embedded Networked Sensor Systems*, 2008, S. 443–444.

[Li13] B. Li, B. Harvey, T. Gallagher: *Using barometers to determine the height for indoor positioning*, *2013 International Conference on Indoor Positioning and Indoor Navigation, IPIN 2013*, 2013.

[Lin15] H. Lin, W. Xu, N. Guan, D. Ji, Y. Wei, W. Yi: *Noninvasive and Continuous Blood Pressure Monitoring Using Wearable Body Sensor Networks*, *IEEE Intelligent Systems*, Bd. 30, Nr. 6, 2015, S. 38–48.

[Lud17] J. Ludikhuize, S. M. Smorenburg, S. E. De Rooij, E. De Jonge: *Rapid response systems. Recognition and management of the deteriorating patient*, *UvA-DARE (Digital Academic Repository) Rapid*, 2017.

[Luo16] N. Luo, W. Dai, C. Li, Z. Zhou, L. Lu, C. C. Poon, S. C. Chen, Y. Zhang, N. Zhao: *Flexible Piezoresistive Sensor Patch Enabling Ultralow Power Cuffless Blood Pressure Measurement*, *Advanced Functional Materials*, Bd. 26, Nr. 8, 2016, S. 1178–1187.

[M. 87] M. Borell: *Instrumentation and the rise of modern physiology*, *Science & Technology Studies*, Bd. 5, 1987, S. 53–62.

[Mah05] S. Z. Mahmoodabadi, A. Ahmadian, M. D. Abolhasani: *Ecg feature extraction using daubechies wavelets*, *Proceedings of the Fifth IASTED International Conference*, Bd. 2, Nr. 2, 2005, S. 343–348.

[Mat10] B. Matt, D. Marshal, D. McCOMBIE: *Body-worn System for Measuring Continuouse Non-invasive Blood pressure (cNIBP)*, 2010.

[McC10a] D. B. McCombie, H. H. Asada, A. T. Reisner: *Calibration of Pulse Transit Time Measurements to Arterial Blood Pressure using External Arterial Pressure Applied along the Pulse Transit Path*, 2010.

[McC10b] D. B. McCombie, A. T. Reisner, H. H. Asada, P. Shaltis: *Wearable pulse wave velocity blood pressure sensor and methods of calibration thereof*, 2010.

[Mih06] E. Mihci, F. Kardelen, B. Dora, S. Balkan: *Orthostatic heart rate variability analysis in idiopathic Parkinson's disease*, *Acta Neurologica Scandinavica*, Bd. 113, Nr. 5, 2006, S. 288–293.

[Muk15] R. Mukkamala, J.-O. Hahn, O. T. Inan, L. K. Mestha, C.-S. Kim, H. Töreyin, S. Kyal: *Towards Ubiquitous Blood Pressure Monitoring via Pulse Transit Time: Theory and Practice*, *IEEE Trans Biomed Eng.*, Bd. 62, Nr. 8, 2015, S. 1879–1901.

[Oh08] H.-H. Oh, B.-C. Shim, G.-S. Kim, Y.-H. Ku, S.-M. Cho, H.-K. Hong: *Apparatus and method for measuring blood pressure*, 2008.

[Owe99] P. Owens, N. Atkins, E. O'Brien: *Diagnosis of white coat hypertension by ambulatory blood pressure monitoring.*, *Journal of American Heart Association*, Bd. 34, Nr. 2, 1999, S. 267–272.

[Pen92] J. Penáz: *Criteria for set point estimation in the volume clamp method of blood pressure measurement*, *Physiological research*, Bd. 41, Nr. 1, 1992, S. 5–10.

[Per93] D. Perloff, C. Grim, J. Flack, E. D. Frohlich, M. Hill, M. McDonald, B. Morgenstern: *AHA Medical / Scientific Statement Human Blood Pressure Determination by Sphygmomanometry*, *Circulation*, Bd. 88, Nr. 5, Pt 1, 1993, S. 2460–2470.

[Pet48] L. H. Peterson, R. D. Dripps, G. C. Risman: *A Method for Recording the Arterial Pressure Pulse and Blood Pressure in Man*, *American heart journal*, 1948.

[Pic05] T. G. Pickering, J. E. Hall, L. J. Appel, B. E. Falkner, J. Graves, M. N. Hill, D. W. Jones, T. Kurtz, S. G. Sheps, E. J. Roccella: *Recommendations for blood pressure measurement in humans and experimental animals: Part 1: Blood pressure measurement in humans - A statement for professionals from the Subcommittee of Professional and Public Education of the American Heart Association Co*, *Circulation*, Bd. 111, Nr. 5, 2005, S. 697–716.

[Poo06] C. C. Y. Poon, Y.-T. Zhang, Y. Liu: *Modeling of Pulse Transit Time under the Effects of Hydrostatic Pressure for Cuffless Blood Pressure Measurements*, *2006 3rd IEEE/EMBS International Summer School on Medical Devices and Biosensors*, 2006, S. 65–68.

[Ric16] R. Richer, B. H. Groh, P. Blank, E. Dorschky, C. Martindale, J. Klucken, B. M. Eskofier: *Unobtrusive real-time heart rate variability analysis for the detection of orthostatic dysregulation*, in *BSN 2016 - 13th Annual Body Sensor Networks Conference*, 2016, S. 189–193.

[Sha08] P. Shaltis, T. Reisner, H. H. Asada: *Cuffless blood pressure monitoring using hydrostatic pressure changes*, *IEEE transactions on bio-medical engineering*, Bd. 55, Nr. 6, 2008, S. 1775–1777.

[Sha17] M. Sharma, K. Barbosa, V. Ho, D. Griggs, T. Ghirmai, S. Krishnan, T. Hsiai, J.-C. Chiao, H. Cao: *Cuff-Less and Continuous Blood Pressure Monitoring: A Methodological Review*, *Technologies*, Bd. 5, Nr. 2, 2017, S. 21.

[Shr10] R. Shriram, A. Wakankar, N. Daimiwal, D. Ramdasi: *Continuous cuffless blood pressure monitoring based on PTT*, *ICBBT 2010 - 2010 International Conference on Bioinformatics and Biomedical Technology*, 2010, S. 51–55.

[Tho16] S. S. Thomas, V. Nathan, C. Zong, K. Soundarapandian, X. Shi, R. Jafari: *BioWatch: A Noninvasive Wrist-Based Blood Pressure Monitor That Incorporates Training Techniques for Posture and Subject Variability*, *IEEE Journal of Biomedical and Health Informatics*, Bd. 20, Nr. 5, 2016, S. 1291–1300.

[Web13] S. Weber, P. Scharfschwerdt, T. Seel, T. Schauer, U. Kertscher, K. Affeld: *Continuouse Wrist Blood Pressure Measurement with Ultrasound*, *Biomed Tech*, Bd. 58, Nr. 1, 2013, S. 24–25.

[Zha11] M. Zhang, A. a. Sawchuk: *A feature selection-based framework for human activity recognition using wearable multimodal sensors*, *Proceedings of the 6th International Conference on Body Area Networks*, 2011, S. 92–98.